

Dr. A.S.Rukhlenko

Design of SPUDT and RSPUDT SAW Filters

Rukhlenko@bluewin.ch

www.intraSAW.com

Neuchâtel, 2005

Outline

Introduction

- 1. Single Phase Unidirectional SAW Transducer (SPUDT)**
- 2. SPUDT Design**
- 3. SPUDT Modeling**
- 4. SPUDT Design and Modeling Example**
- 5. RSPUDT Optimization**

Conclusions

Introduction

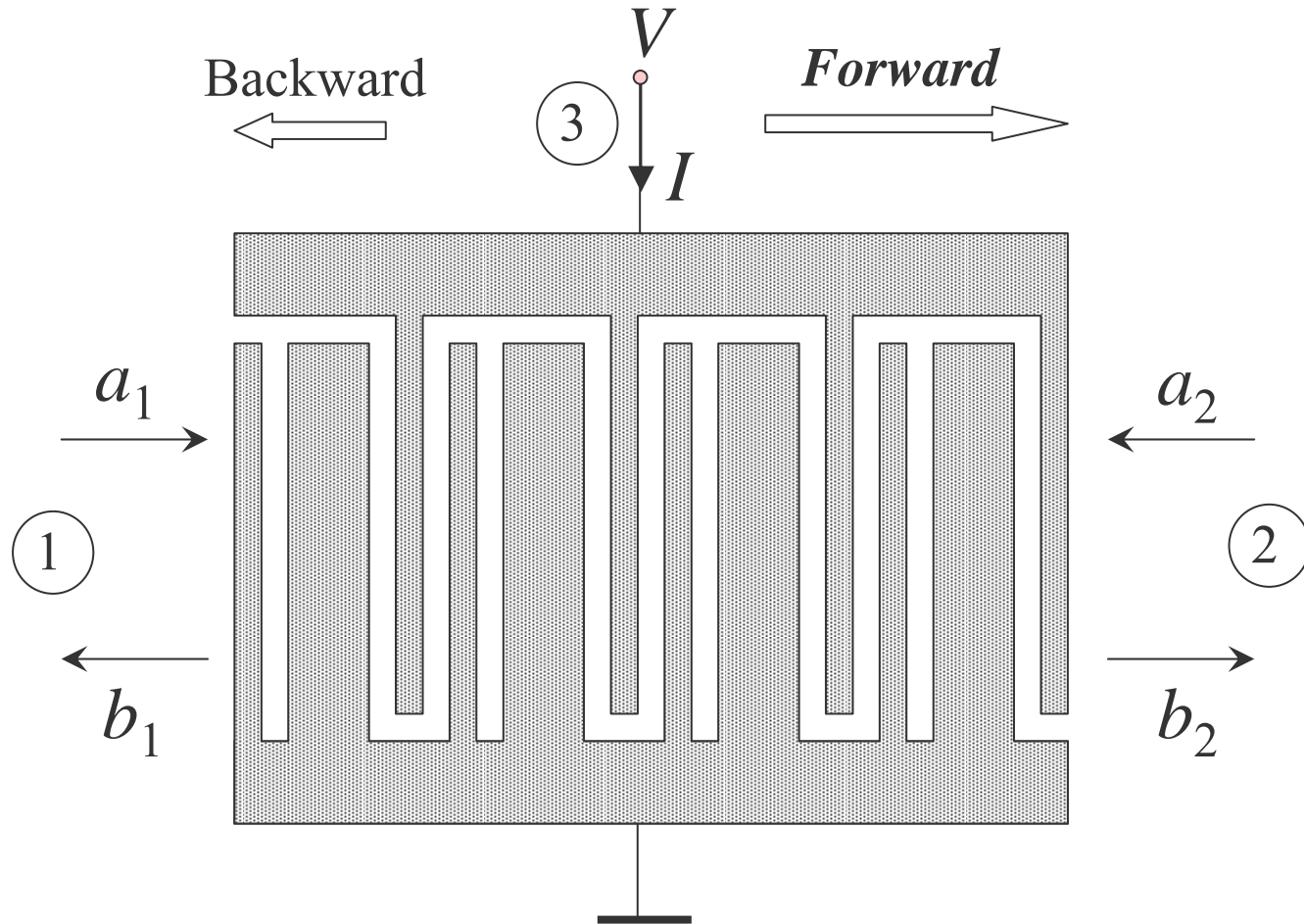


Fig. 1. SPUDT three-port representation and directivity

SAW Transducer Modeling

Mixed scattering matrix (P-matrix)

$$\begin{bmatrix} b_1 \\ b_2 \\ I_3 \end{bmatrix} = \begin{bmatrix} m_{11} & m_{12} & m_{13} \\ m_{21} & m_{22} & m_{23} \\ m_{31} & m_{32} & m_{33} \end{bmatrix} \begin{bmatrix} a_1 \\ a_2 \\ V_3 \end{bmatrix} \quad (1)$$

Wave scattering matrix (S-matrix)

$$\begin{bmatrix} b_1 \\ b_2 \\ b_3 \end{bmatrix} = \begin{bmatrix} s_{11} & s_{12} & s_{13} \\ s_{21} & s_{22} & s_{23} \\ s_{31} & s_{32} & s_{33} \end{bmatrix} \begin{bmatrix} a_1 \\ a_2 \\ a_3 \end{bmatrix} \quad (2)$$

where a_i, b_i $i=1, 2$ are amplitudes of the incident and reflected waves at the acoustical ports 1, 2 and I_3, V_3 are current and terminal voltage at the electrical port 3.

Conversion between P- and S-matrices

Wave and electrical variables are interrelated

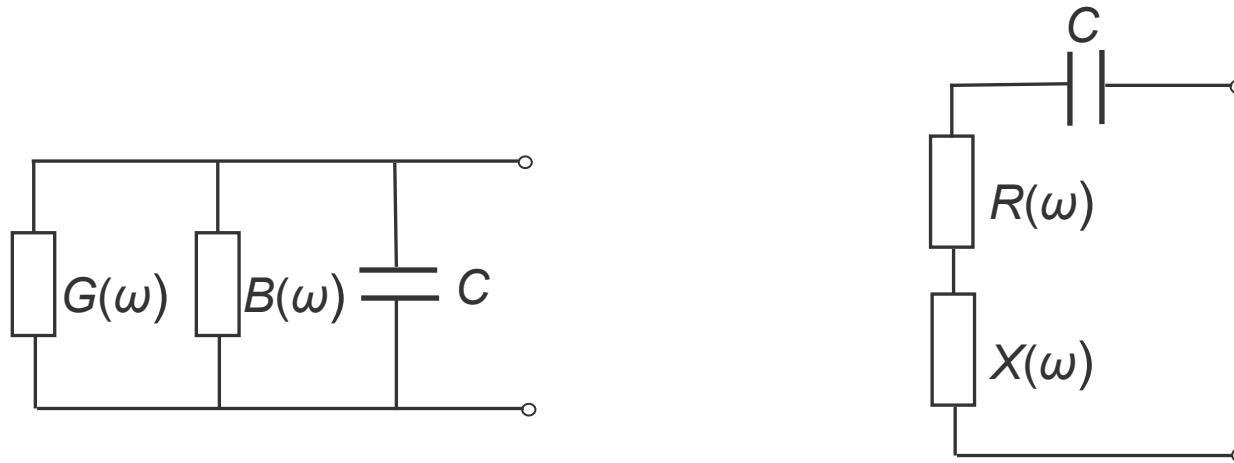
$$\begin{aligned} a_i &= \frac{1}{2} \left(\sqrt{Z_i} I_i + \sqrt{Y_i} V_i \right) \\ b_i &= \frac{1}{2} \left(\sqrt{Z_i} I_i - \sqrt{Y_i} V_i \right) \end{aligned}, \quad i=1,2,3 \quad (3)$$

where $Z_i=1/Y_i$ is the characteristic admittance at the i -th port, $i=1,2,3$.

$$\mathbf{S} = \begin{bmatrix} S_{11} & S_{12} & S_{13} \\ S_{21} & S_{22} & S_{23} \\ S_{31} & S_{32} & S_{33} \end{bmatrix} = \begin{bmatrix} m_{11} - \frac{m_{13}m_{31}}{Y_0 + Y} & m_{12} - \frac{m_{13}m_{32}}{Y_0 + Y} & \frac{2\sqrt{Y_0}m_{13}}{Y_0 + Y} \\ m_{21} - \frac{m_{23}m_{31}}{Y_0 + Y} & m_{22} - \frac{m_{23}m_{32}}{Y_0 + Y} & \frac{2\sqrt{Y_0}m_{23}}{Y_0 + Y} \\ -\frac{\sqrt{Y_0}m_{31}}{Y_0 + Y} & -\frac{\sqrt{Y_0}m_{32}}{Y_0 + Y} & \frac{Y_0 - m_{33}}{Y_0 + Y} \end{bmatrix} \quad (4)$$

where $Y=G(\omega)+jB(\omega)+j\omega C$ is the transducer admittance, C is the static capacitance, Y_0 is the load admittance.

SAW Transducer Equivalent Scheme



a) Parallel: $Y(\omega) = G(\omega) + jB(\omega) + j\omega C$ b) Series: $Z(\omega) = R(\omega) + jX(\omega) + (j\omega C)^{-1}$

Fig. 2. Equivalent scheme

Radiation conductance $G(\omega) = \text{Re} \{m_{33}(\omega)\} = |m_{13}|^2 + |m_{23}|^2$ (5)

Radiation susceptance $B(\omega) = H \{G(\omega)\} = \frac{1}{\pi} \int_{-\infty}^{\infty} \frac{G(\omega')}{\omega - \omega'} d\omega'$ (6)

C is the static capacitance (electrostatic problem solution)

Transducer Reflectivity

The net reflection coefficient at the i -th acoustic port

$$s_{ii} = m_{ii} + \Delta m_{ii}, \quad i = 1, 2 \quad (7)$$

m_{ii} – mechanical (mass-electrical load - MEL) reflection coefficient (s.c. $V=0$)

Δm_{ii} – regenerated reflection coefficient (electrical termination, $V \neq 0$)

$$\Delta m_{ii} = -\frac{m_{i3}m_{3i}}{Y_0 + Y} \quad (8)$$

The larger value of the net reflection coefficient s_{ii} , the larger amplitude of the triple transit echo (TTE) signal (multiple transit inter-transducer SAW reflections superimposed on the main signal).

Minimum net reflection condition (classical bidirectional transducer):

- 1) low MEL reflection $|m_{ii}| \ll 1$ (ideally zero),
- 2) short circuit $Y_0 \rightarrow \infty \implies s_{ii} \rightarrow 0$.

Transducer Transmission

The transmission function at the i -th acoustic port

$$s_{i3} = \frac{2\sqrt{Y_0} m_{i3}}{Y_0 + Y} \quad (9)$$

Maximum transmission condition (bidirectional transducer):
open circuit $Y_0 \rightarrow 0$.

Minimum reflection (low TTE) and maximum transmission and/or low insertion loss (IL) requirements are contraversary.

A trade-off between TTE and IL must be attained by using the appropriate design and matching, in general case.

Single Phase Unidirectional SAW Transducer (SPUDT)

Key Idea:

Pass band compensation of the regenerated term Δm_{ij} by the mechanical reflection function m_{ij} , with the both terms having substantially large amplitudes.

Design Goal:

By synthesizing the reflectivity function (discrete set of the realizable SPUDT finger reflection coefficients) and the excitation function (withdrawal-weighted acoustical sources) to meet simultaneously:

- 1) specifications on the desired (target) SPUDT frequency response
- 2) small net reflection coefficient at the forward acoustical port.

Basic SPUDT Properties

1. Contrary to bidirectional SAW transducers, SPUDT deliberately includes internal mechanical reflections in a way to cancel the effect of the regenerated reflections at one of the acoustic ports (forward or backward), so that the net reflection coefficient almost vanishes in the pass band if the device is properly matched.
2. This can be done by appropriate selection of the electrical load and by weighting the reflection function.
3. Due to a small value of the net reflection coefficient at the internal (acoustically coupled) ports the triple transit echo is well suppressed in SPUDT SAW filters.
4. The valuable by-product of the low-level TTE in addition to the small passband ripple is the low insertion loss in the matched SPUDT SAW filter.

Acoustoelectric Conversion and Reflection

For a lossless and reciprocal SPUDT, the mixed scattering matrix elements satisfies a self-consistent system of equations¹

$$\begin{cases} m_{13}^* = -(m_{23} + rm_{23}^*) / t \\ m_{23}^* = -(m_{13} + rm_{13}^*) / t \\ rr^* + tt^* = 1 \\ rt^* + tr^* = 0 \end{cases} \quad (6)$$

$m_{13} = -m_{31}/2$ acoustoelectric function in the backward direction

$m_{23} = -m_{32}/2$ acoustoelectric function in the forward direction

$r = m_{11} = m_{22}$ SPUDT reflection coefficient

$t = m_{12} = m_{21}$ SPUDT transmission coefficient.

Zero Reflection Condition:
$$m_{ii} = \frac{m_{i3}m_{3i}}{Y_0 + Y} = -\frac{2m_{i3}^2}{Y_0 + Y}, \quad i = 1, 2 \quad (7)$$

Reflection and Transduction Centers

The **reflection center** (RC) stands for the reference plane position at which the reflection coefficient (local or global) is pure imaginary.

The **transduction (excitation) center** (TC) is referred to the position of the reference plane where two waves radiated in the forward and backward direction are in-phase.

In many practical cases, the reflection and transduction centers are related directly with the geometrical centers of symmetry for a short-circuit transducer (mechanical reflections) and for a reflectionless “live” transducer (transduction), with finger potentials taken into account.

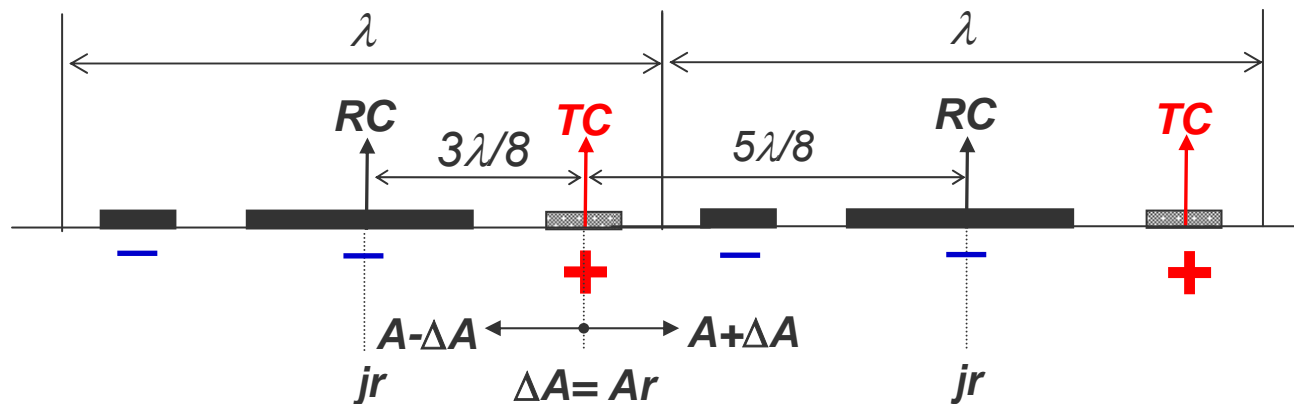


Fig. 3. DART reflection and transduction centers and wave interference

SPUDT Directivity

The directivity function

$$D = \frac{|m_{13}|^2 - |m_{23}|^2}{|m_{13}|^2 + |m_{23}|^2} \quad (8)$$

that is the fractional difference of power radiated in each direction with respect to the total power radiated in both directions.

If we define Φ as the phase difference between RC and TC, the phase difference 2Φ between m_{13} and m_{23} follows from Eq. (6).

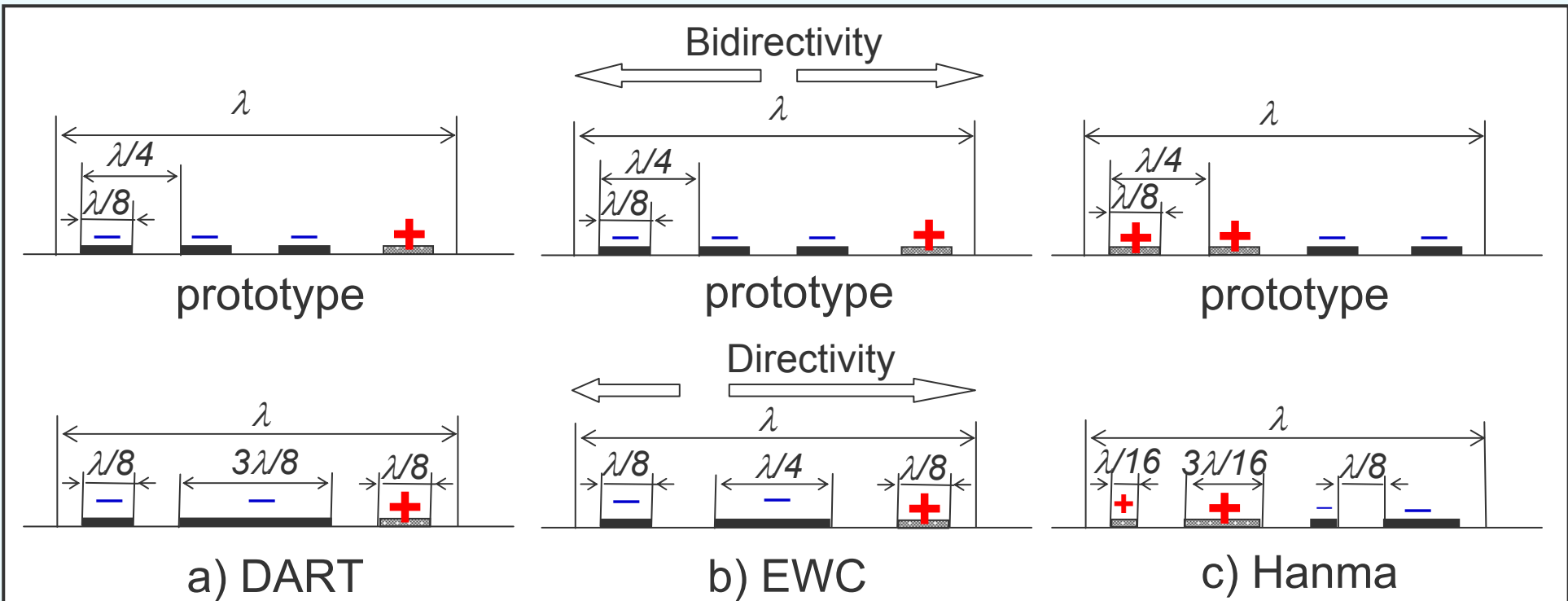
It can be deduced from (8) using the properties (6) that

- 1) $D=0$ (bidirectionality) if
 - $\Phi=0$ (symmetric SAW excitation) or
 - $\Phi=\pm\pi/2$ (antisymmetric SAW excitation)
 - 2) $0 < |D| \leq 1$ (unidirectionality) if
 - $\Phi=\pm\pi/4+n\pi$
 - 3) $|D|=1$ (ideal unidirectionality) if $|r|=1$, $\Phi=\pm\pi/4+n\pi$.
- (9)

Global and Local Directivity

1. We shall refer to **global** RC and transduction TC centers as for the overall SPUDT reflection and transductions functions.
2. We shall refer to **local** RC and TC as for the elemental SPUDT cells (DART, EWC, etc.).
3. **Global Directivity Condition:** Phase shift between the global RC and TC must satisfy Eq. (9).
4. **Local Directivity Condition:** Phase shift between the local RC and TC must satisfy Eq (9) for each reflective elemental SPUDT cell.
5. **Directivity implementation:** In SPUDT structures (DART, EWC, etc.), directivity is obtained by the physical separation of the global or local RC and TC by the distance $l = \pm\lambda/8 + n\lambda/2$.

Basic SPUDT Cell Types



DART - **D**istributed **A**coustic **R**eflector **T**ransducer

EWC - **E**lectrode **W**idth **C**ontrolled transducer

Hanma - transducer proposed by K. Hanma and B. Hunsinger (1976)

Fig. 4. Basic SPUDT cells

DART/EWC Properties

1. DART structure is obtained by “filling in” the gap between second and third electrodes in the prototype cell.
2. The DART has a transduction center approximately at the center of the “hot” finger ($\Delta\Phi\approx 1.2^\circ$), with a reflection center placed located exactly in the center of the wide reflective electrode.
3. In the EWC, there are more distortion of the electrostatic field that causes the larger transduction phase discrepancy ($\Delta\Phi\approx -3.9^\circ$). The reflection coefficient is expected to be smaller if compared to the DART.
4. Both DART and EWC have the harmonic responses at the frequencies $2\omega_0$ and $3\omega_0$ where ω_0 is the IDT central frequency.

Hanma Properties

1. A Hanma structure is obtained by changing alternatively the electrode width in the split-finger prototype transducer from $\lambda/8$ to $\lambda/16$ and $3\lambda/16$. This structure has the largest discrepancy both in transduction and reflection phase. The merit of the structure is the higher transduction efficiency as it has two “hot “ fingers of different width in the cell.
2. The Hanma SPUDT has the harmonic response at the frequency $3\omega_0$ (like a bidirectional split-finger SAW transducer), with no harmonic at ω_0 that may be of importance in some applications.
3. The Hanma structure is impractical in high-frequency SAW filters as it contains narrow fingers of width $\lambda/16$.

Resonant SPUDT (RSPUDT)

A SPUDT with both the positive and negative reflections while maintaining the global directivity is known as a resonant SPUDT, or RSPUDT, as two reflectors of different signs give a weak resonance in the passband.

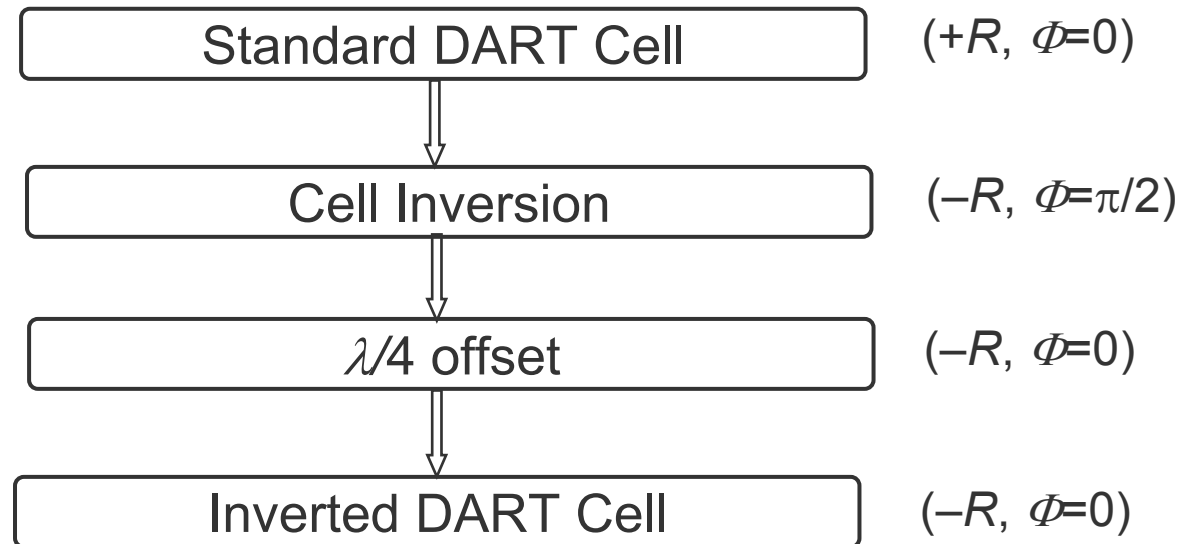


Fig. 5. DART conversion with positive/negative reflectivity

RSPUDT Cells

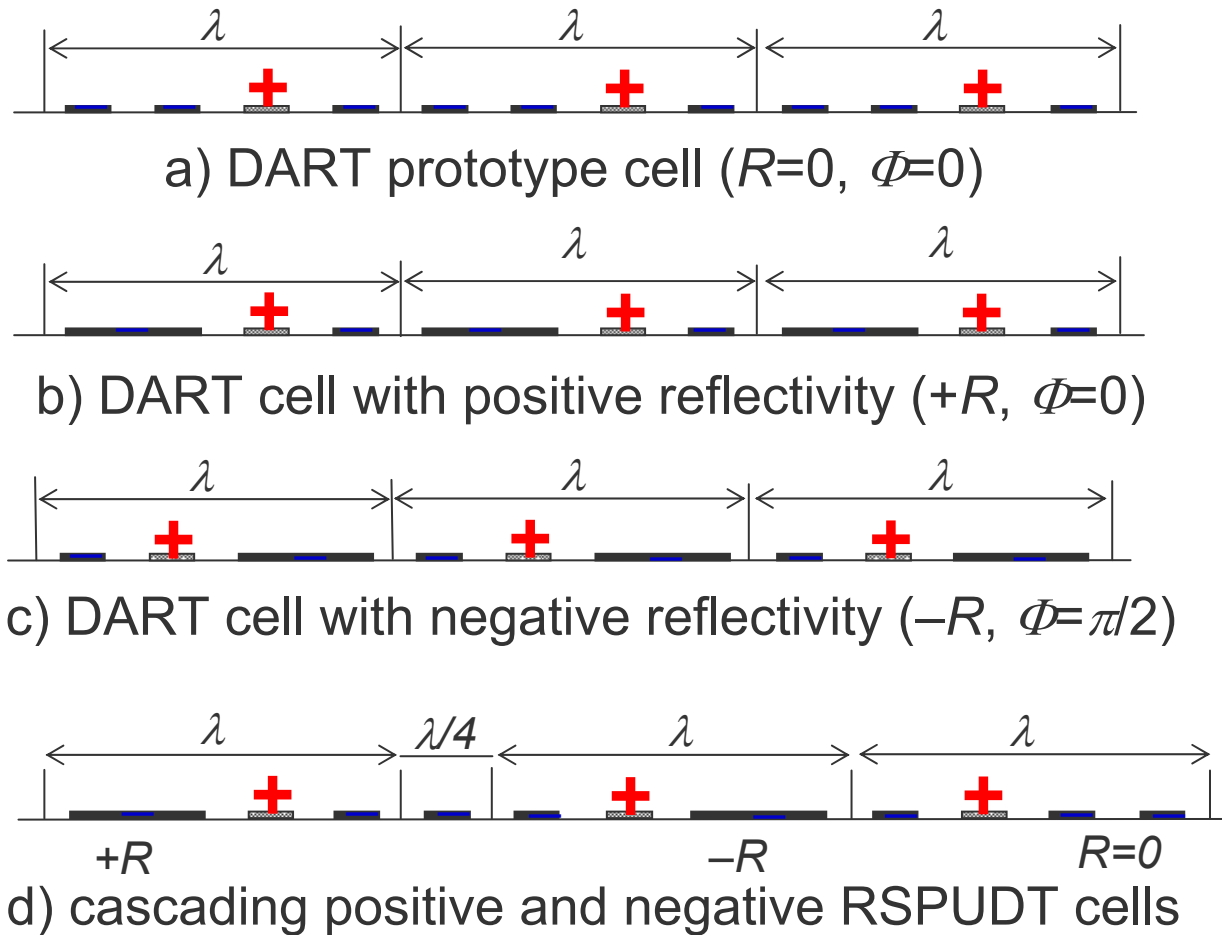
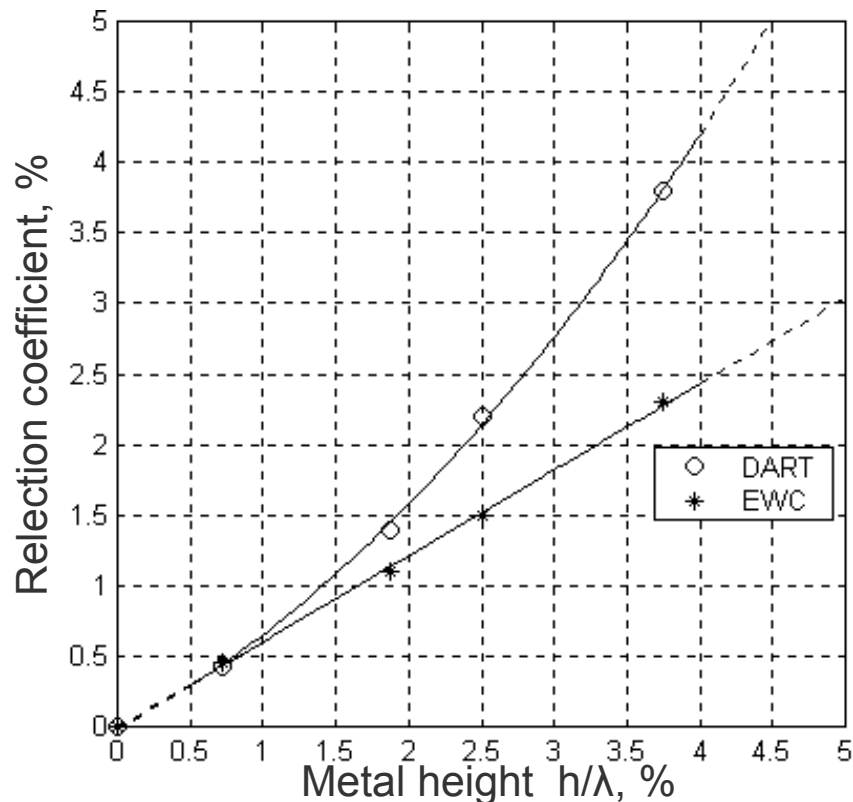


Fig. 6. RSPUDT structures with positive and negative reflectivity

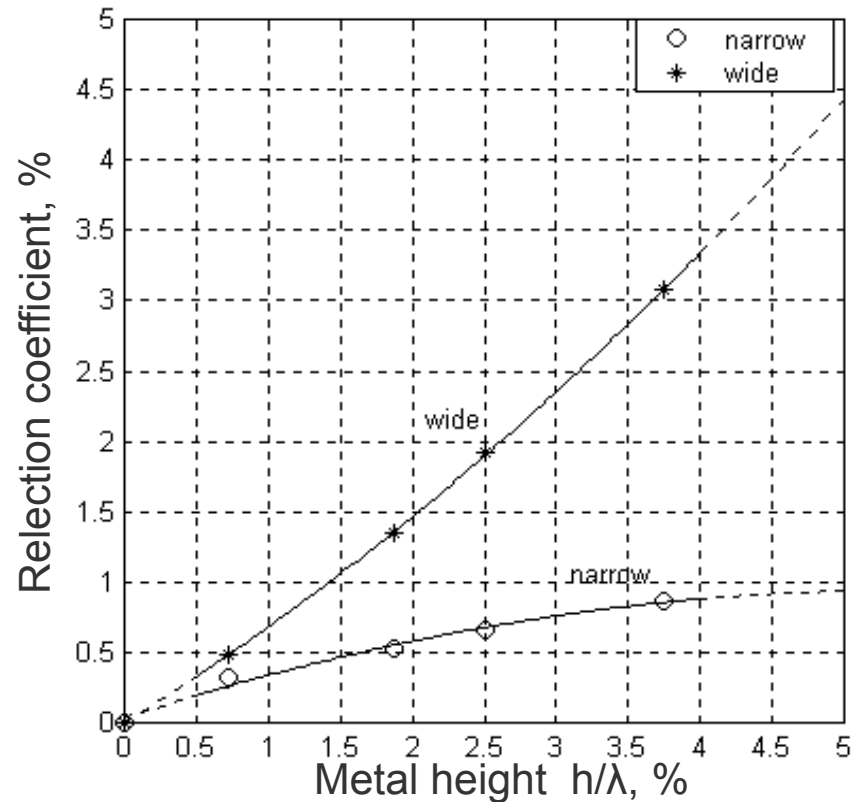
RSPUDT Properties

1. For given specifications, RSPUDT designs result in the most compact filter size.
2. RSPUDT improve SAW filter performance (IL, pass band ripple, shape factor) if compared to the classical SPUDT.
3. RSPUDT design is sophisticated and time consuming as the non-linear programming must be applied to optimization of both the reflective and transduction functions.

SPUDT Cell Reflection Coefficient



a) DART and EWC



b) Hanma's SPUDT

Fig. 6 Reflection coefficient of the SPUDT elemental cells vs metal thickness (substrate material 38° YX quartz)

Classical SPUDT Design

Design Goal

A perfect unidirectionality is not the key design goal in SPUDT filters. Rather, the major goal is achieving low (ideally zero) reflection at the forward acoustic port under the condition of a *good impedance matching* on the electrical port.

A well-designed classical SPUDT simultaneously achieves:

- 1) low triple transit echo
- 2) low insertion loss.

Synthesis Goal

Contrary to conventional bidirectional SAW filters, both the weighted transduction (SAW excitation) function and the weighted reflection function are to be synthesized to meet a self-consistent set of M_{11} , M_{13} and M_{33} such that

- 1) $S_{22} \approx 0$ under matched conditions (forward directivity to the right direction)
- 2) S_{23} provides the desired magnitude and phase (or group delay) response of a single SPUDT transducer.

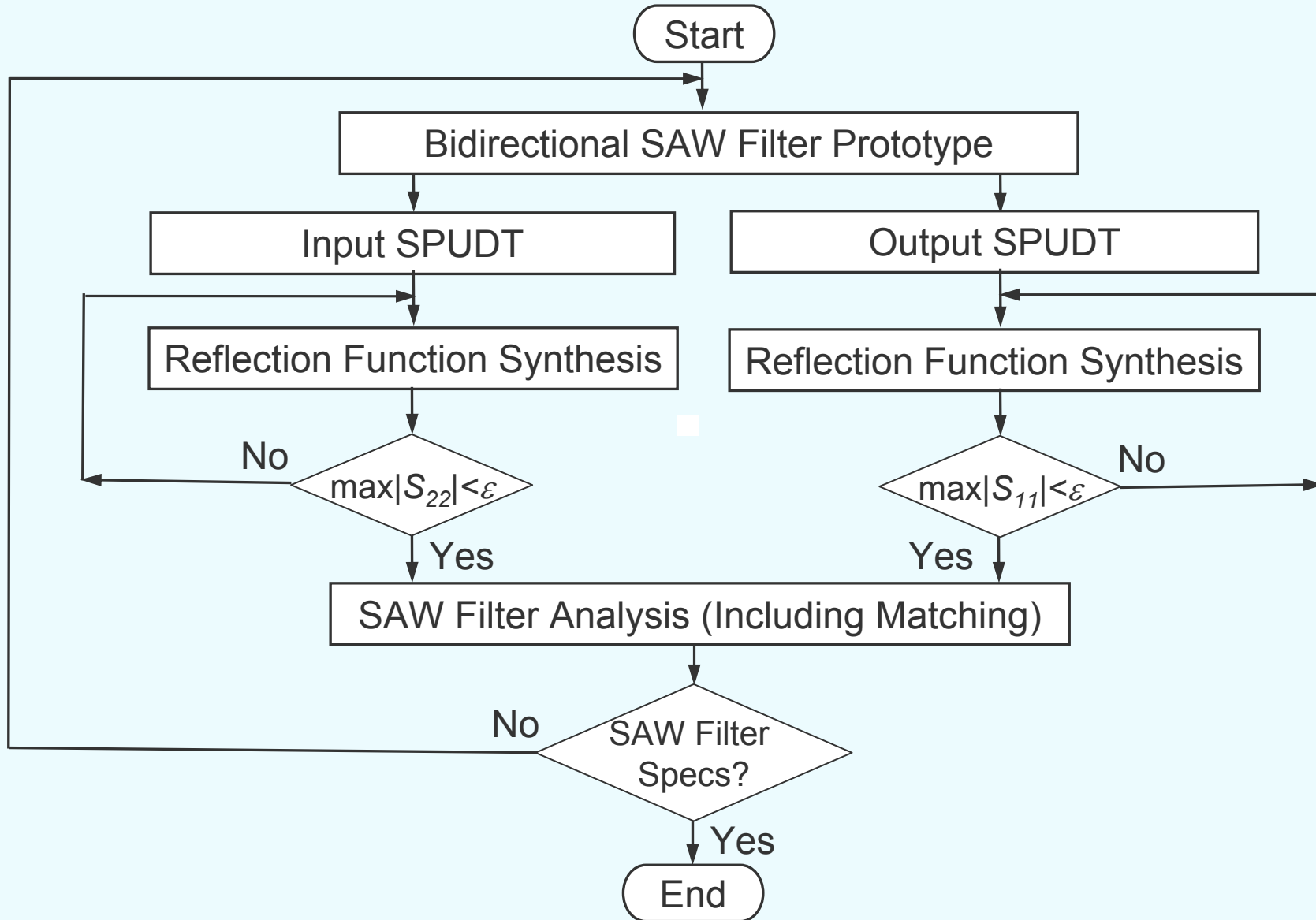
Design Features

1. A principal design problem is that the presence of the reflections modifies M_{13} and M_{33} which in turn affect the regeneration function. Therefore, the reflection function synthesis is aiming at a moving target and should be done iteratively, in general case.
2. A second problem is that the transduction tap weights are no longer related to the transduction function in the frequency domain via the Fourier transform due to the presence of the mechanical reflections which significantly distort the SPUDT time (impulse) response if compared to the reflectionless bidirectional SAW transducer.

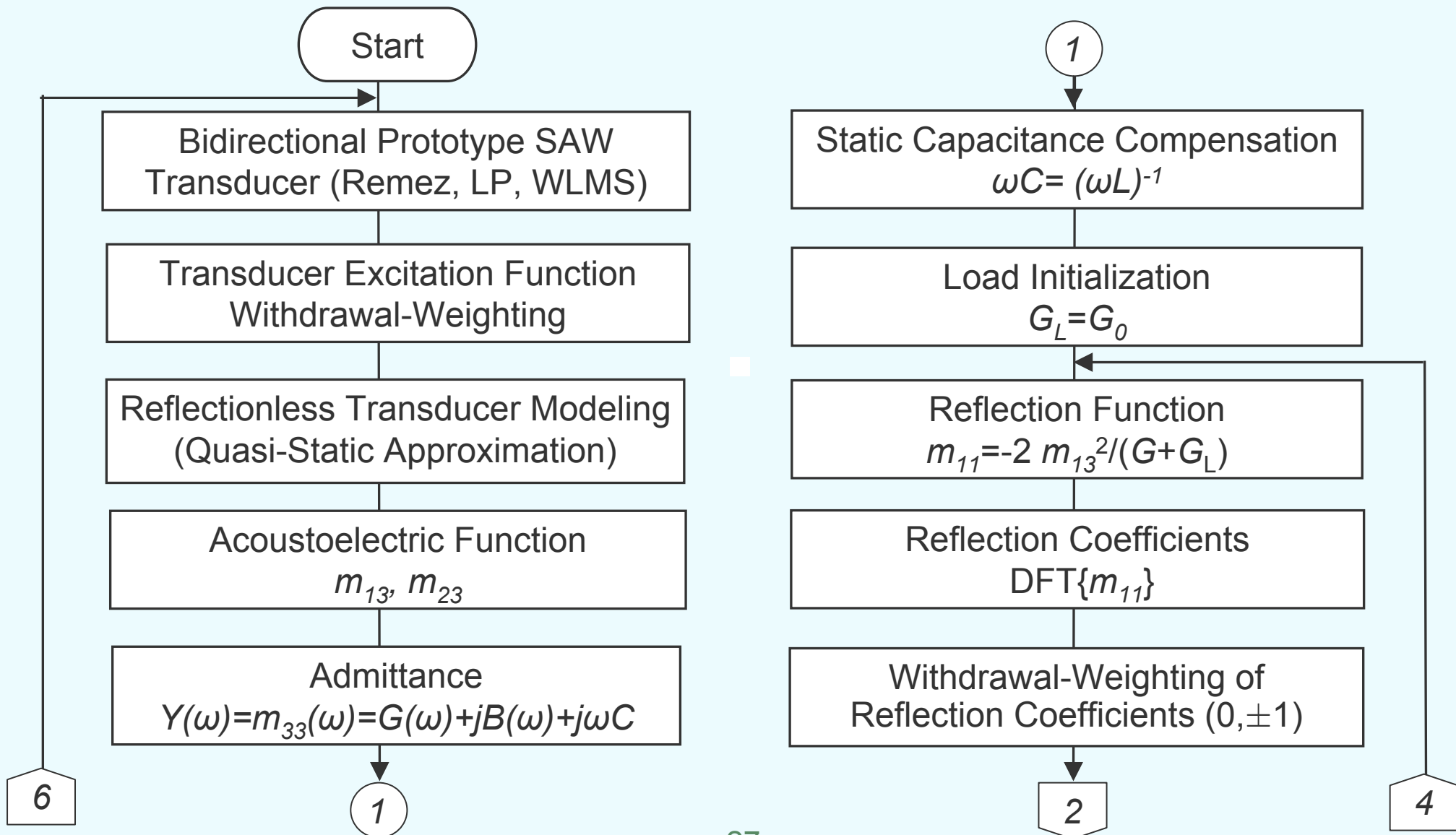
Assumptions and Simplifications

1. Weak reflectivity of a SPUDT cell is supposed so that to the first order the reflectivity function is related by the Fourier transform with the transducer reflection coefficient M_{22} .
2. In the simulation, the imaginary part of the transducer admittance $\text{Im}\{Y(\omega)\}=B(\omega)+\omega C$ is compensated in the passband by a simple matching circuit, typically a parallel inductor.
- 3) Admittance $|Y_0+Y|\approx\text{const}$ in the passband so that the shape of the M_{22} weakly depends on the transducer admittance Y and the electrical load Y_0 .
4. Resistive losses which significantly contribute to the SPUDT filter insertion loss can be separated and modeled by a series lumped resistors at the input and output.
5. Reflection coefficient of the reflective fingers in SPUDT cells is specified a priori.
6. To the first order, $M_{22}\sim -M_{23}^2$ and therefore the reflectivity function can be found as auto-convolution of the transduction function in the time domain.

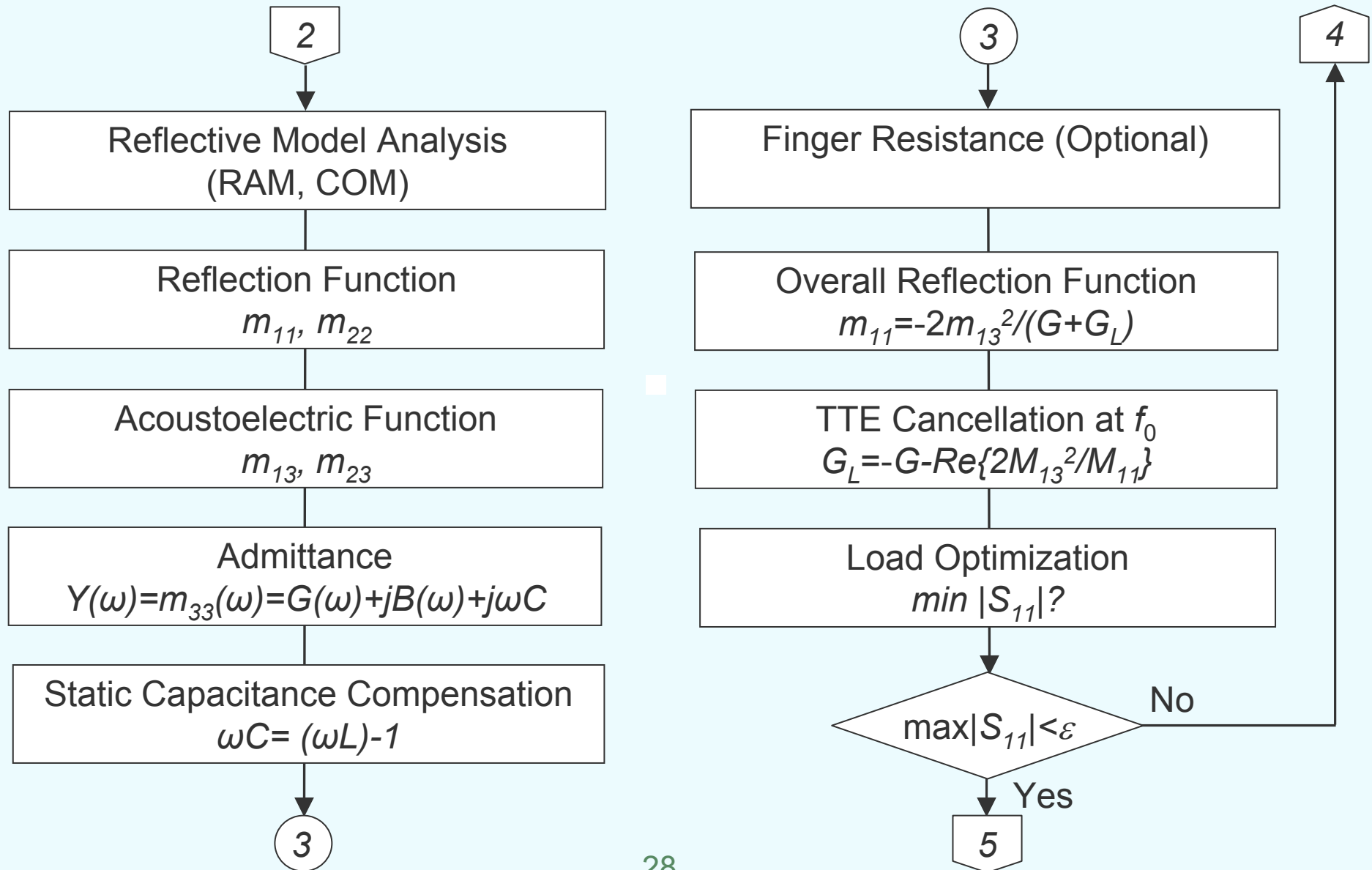
Iterative SPUDT Filter Design Algorithm



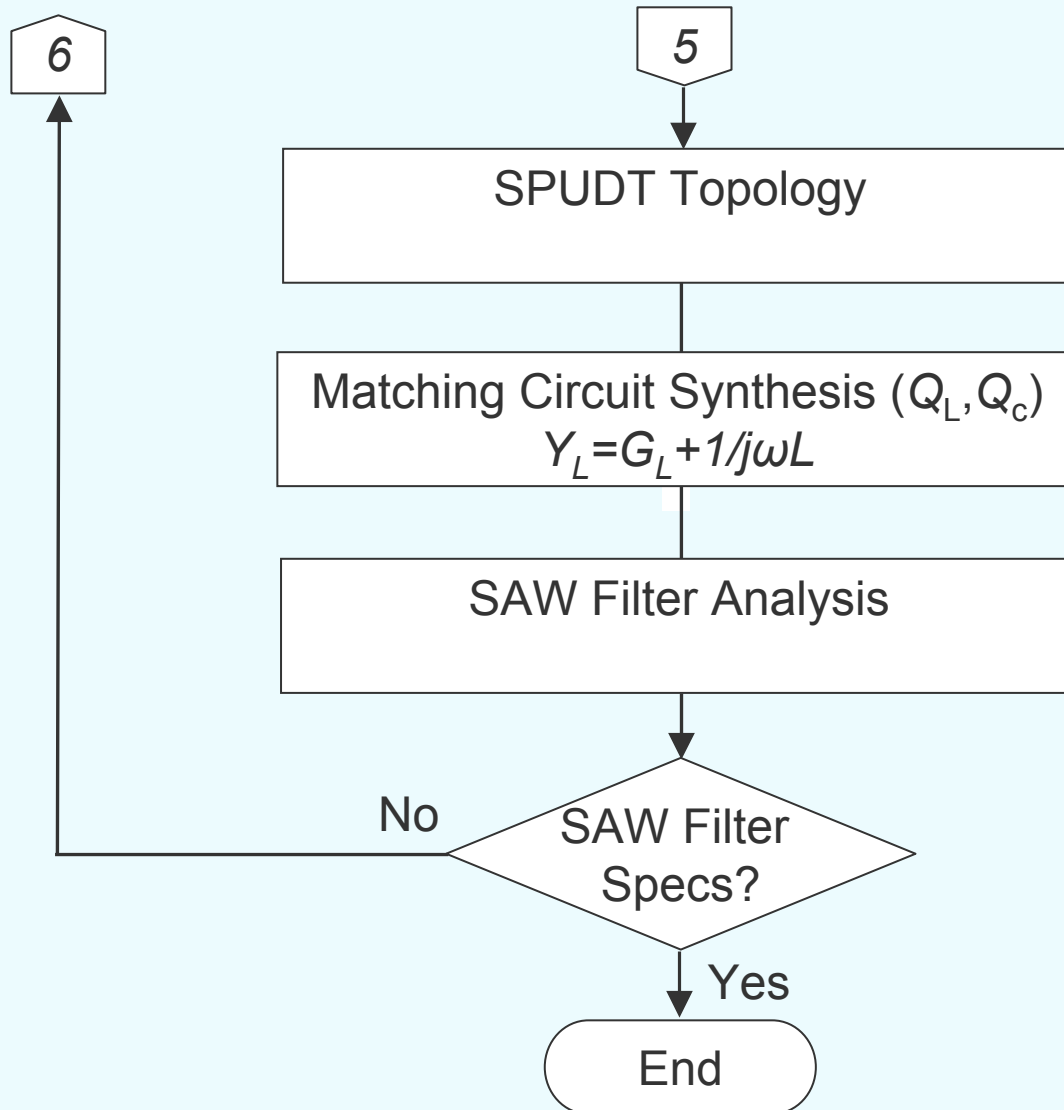
SPUDT Synthesis Algorithm Flowchart



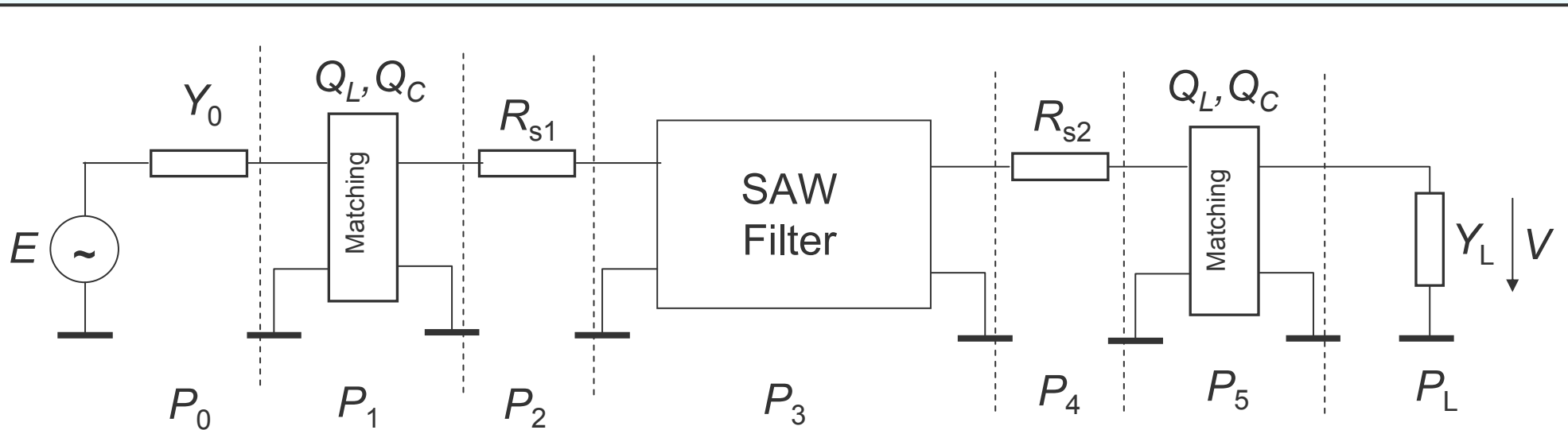
SPUDT Synthesis Algorithm Flowchart (Cont'd)



SPUDT Synthesis Algorithm Flowchart (Cont'd)



Insertion Loss Separation



Y_0 – source admittance

Y_L – load admittance

P_i – electrical power at the i -th stage

P_0 – power available from the source

P_L – power delivered to the load

Fig. 7. Insertion loss segregation for a SAW filter

Insertion Loss Analysis

$$IL = \frac{P_L}{P_{\max}} = \frac{P_0}{P_{\max}} \frac{P_1}{P_0} \frac{P_2}{P_1} \frac{P_3}{P_2} \frac{P_4}{P_3} \frac{P_5}{P_4} \frac{P_L}{P_5} \quad (10)$$

$P_{\max} = 1/8 |E|^2 \operatorname{Re}\{Y_0\}$ maximum delivered power

$P_0 = 1/2 |E|^2 \operatorname{Re}\{Y_0\}$ power available from the generator

$P_L = 1/2 |V|^2 \operatorname{Re}\{Y_L\}$ power delivered to the load

P_0/P_{\max} mismatch losses at the generator end

P_1/P_0 resistive losses in the input matching circuit (Q_L, Q_C)

P_2/P_1 resistive losses in the input SAW transducer

P_3/P_2 conversion losses in SAW filter

P_4/P_3 resistive losses in the output SAW transducer

P_5/P_4 resistive losses in the output SAW transducer (Q_L, Q_C)

P_L/P_5 mismatch losses at the load end

SPUDT Modeling

Algorithm: Recurrent cascading of the elemental reflective/non-reflective cells in terms of the mixed transmission matrices.

In general case, SPUDT can be separated into the following typical regions to be analyzed:

- 1) both reflection and transduction (unidirectional SPUDT cells)
- 2) transduction only (split-finger cells, for example)
- 3) reflections only (short-circuit array)
- 4) neither reflection, no transduction (split-finger short-circuit cells).

Each region can be modeled by using the most relevant model (quasi-static approximation, RAM, COM, etc.) with model parameters tailored for each particular case.

Cascading SPUDT Cells

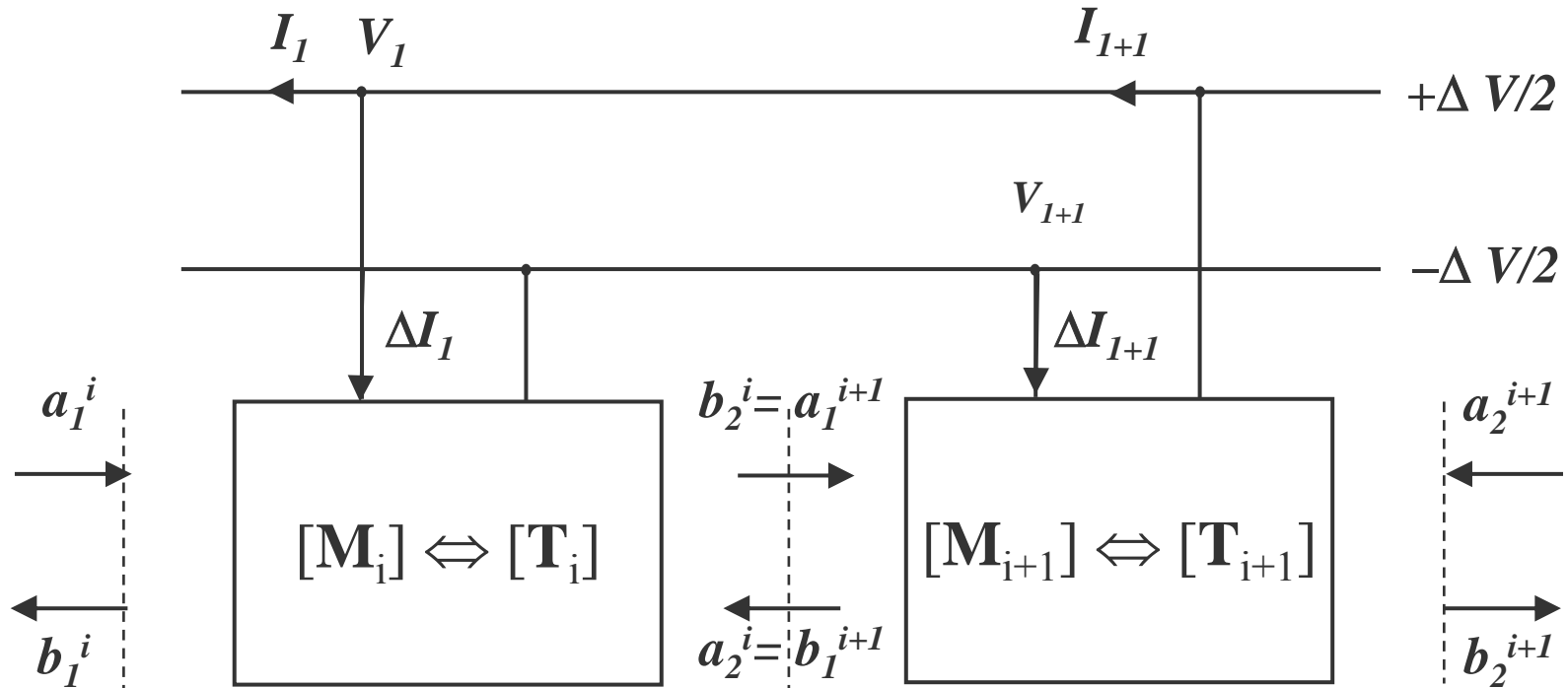


Fig. 8. Cascading of the i -th and $(i+1)$ -th elemental cells

Recurrent Cascading Algorithm

1. *Mixed scattering matrix (P-matrix) of the i -th elemental cell*

$$\begin{bmatrix} b_1^i \\ b_2^i \\ I^i \end{bmatrix} = \begin{bmatrix} m_{11}^i & m_{12}^i & m_{13}^i \\ m_{21}^i & m_{22}^i & m_{23}^i \\ m_{31}^i & m_{32}^i & m_{33}^i \end{bmatrix} \begin{bmatrix} a_1^i \\ a_2^i \\ V^i \end{bmatrix} \quad (11)$$

2. *Conversion to the mixed transmission matrix*

$$\begin{bmatrix} a_1^i \\ b_1^i \\ I^i \end{bmatrix} = \begin{bmatrix} t_{11}^i & t_{12}^i & t_{13}^i \\ t_{21}^i & t_{22}^i & t_{23}^i \\ t_{31}^i & t_{32}^i & t_{33}^i \end{bmatrix} \begin{bmatrix} a_2^i \\ b_2^i \\ V^i \end{bmatrix} = \begin{bmatrix} \frac{1}{m_{21}^i} & -\frac{m_{22}^i}{m_{21}^i} & -\frac{m_{23}^i}{m_{21}^i} \\ \frac{m_{11}^i}{m_{21}^i} & m_{12}^i - \frac{m_{11}^i m_{22}^i}{m_{21}^i} & m_{13}^i - \frac{m_{11}^i m_{23}^i}{m_{21}^i} \\ \frac{m_{31}^i}{m_{21}^i} & m_{32}^i - \frac{m_{22}^i m_{31}^i}{m_{21}^i} & m_{33}^i - \frac{m_{31}^i m_{23}^i}{m_{21}^i} \end{bmatrix} \begin{bmatrix} a_2^i \\ b_2^i \\ V^i \end{bmatrix} \quad (12)$$

Recurrent Cascading Algorithm (Cont'd)

3. Augmented transmission matrix

$$\begin{bmatrix} a_1^i \\ b_1^i \\ V^i \\ I^i \end{bmatrix} = \begin{bmatrix} t_{11}^i & t_{12}^i & p_i t_{13}^i & 0 \\ t_{21}^i & t_{22}^i & p_i t_{23}^i & 0 \\ 0 & 0 & 1 & 0 \\ p_i t_{31}^i & p_i t_{32}^i & t_{33}^i & 1 \end{bmatrix} \begin{bmatrix} a_1^{i+1} \\ b_1^{i+1} \\ V^{i+1} \\ I^{i+1} \end{bmatrix} \quad (13)$$

where $p_i = V_i / \Delta V$ is finger polarity function.

4. Overall transmission matrix for a SAW transducer of N electrodes

$$\mathbf{T} = \mathbf{T}_1 \mathbf{T}_2 \dots \mathbf{T}_N = \begin{bmatrix} T_{11} & T_{12} & T_{13} & 0 \\ T_{21} & T_{22} & T_{23} & 0 \\ 0 & 0 & 1 & 0 \\ T_{31} & T_{32} & T_{33} & 1 \end{bmatrix} \quad (14)$$

Recurrent Cascading Algorithm (Cont'd)

5. Overall mixed scattering matrix

$$\begin{bmatrix} b_1 \\ b_2 \\ I \end{bmatrix} = \begin{bmatrix} M_{11} & M_{12} & M_{13} \\ M_{21} & M_{22} & M_{23} \\ M_{31} & M_{32} & M_{33} \end{bmatrix} \begin{bmatrix} a_1 \\ a_2 \\ V \end{bmatrix} \quad (15)$$

$$\mathbf{M} = \begin{bmatrix} M_{11} & M_{12} & M_{13} \\ M_{21} & M_{22} & M_{23} \\ M_{31} & M_{32} & M_{33} \end{bmatrix} = \begin{bmatrix} \frac{T_{21}}{T_{11}} & T_{22} - \frac{T_{12}T_{21}}{T_{11}} & T_{23} - \frac{T_{21}T_{13}}{T_{11}} \\ \frac{1}{T_{11}} & -\frac{T_{12}}{T_{11}} & -\frac{T_{13}}{T_{11}} \\ \frac{T_{31}}{T_{11}} & T_{32} - \frac{T_{12}T_{31}}{T_{11}} & T_{33} - \frac{T_{13}T_{31}}{T_{11}} \end{bmatrix} \quad (16)$$

Design and Simulation Example

SPUDT SAW Filter Specifications

CDMA SAW filter (DART), LG, 1998

$f_0=85.38$ MHz

Substrate material *ST*-quartz

Metal (aluminum) thickness 3900 Å

Package size 19 x 5 mm

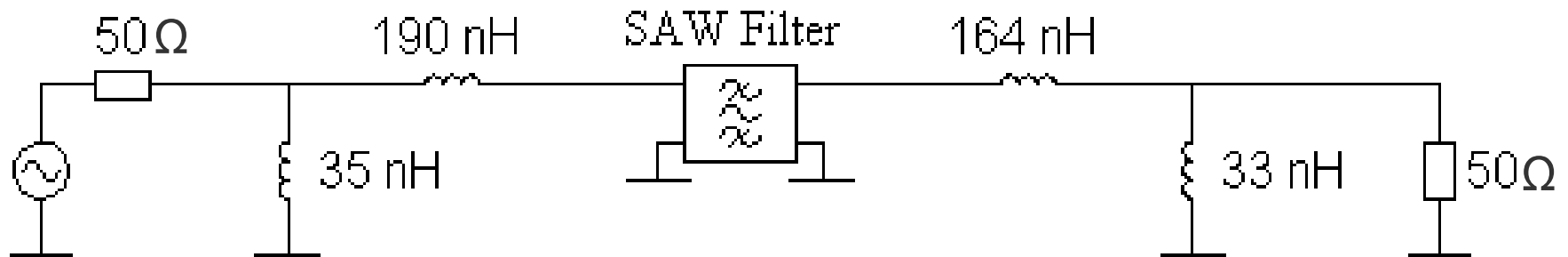
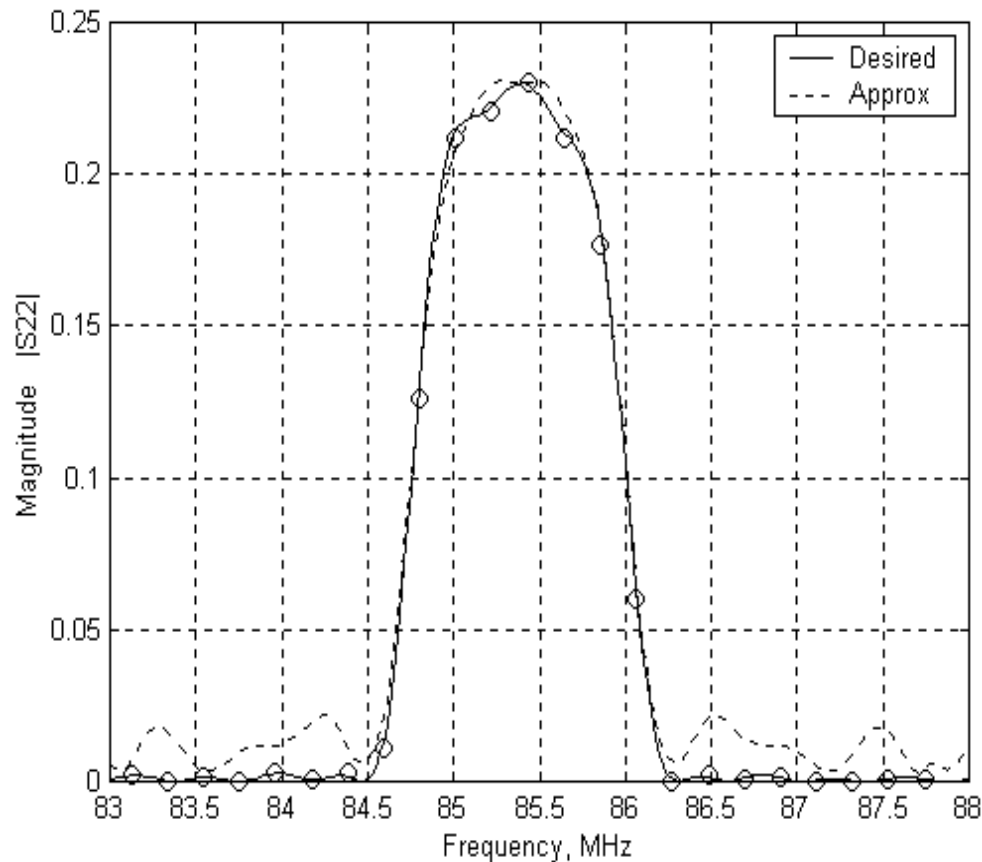
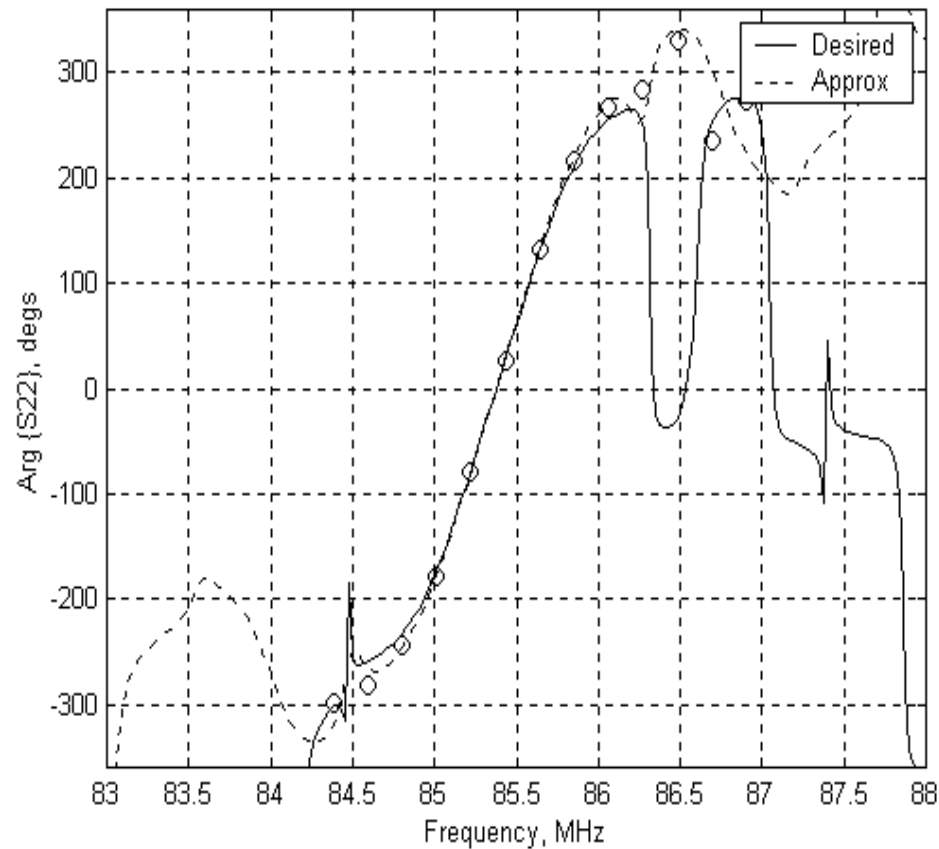


Fig. 9. Matching circuit configuration (computer simulation) using the measured *S*-parameters (inductor $Q=40$)

Input SPUDT: Reflection



a) magnitude



b) phase

Fig. 10. Reflection function (input SPUDT)

Input SPUDT: Scattering Parameters

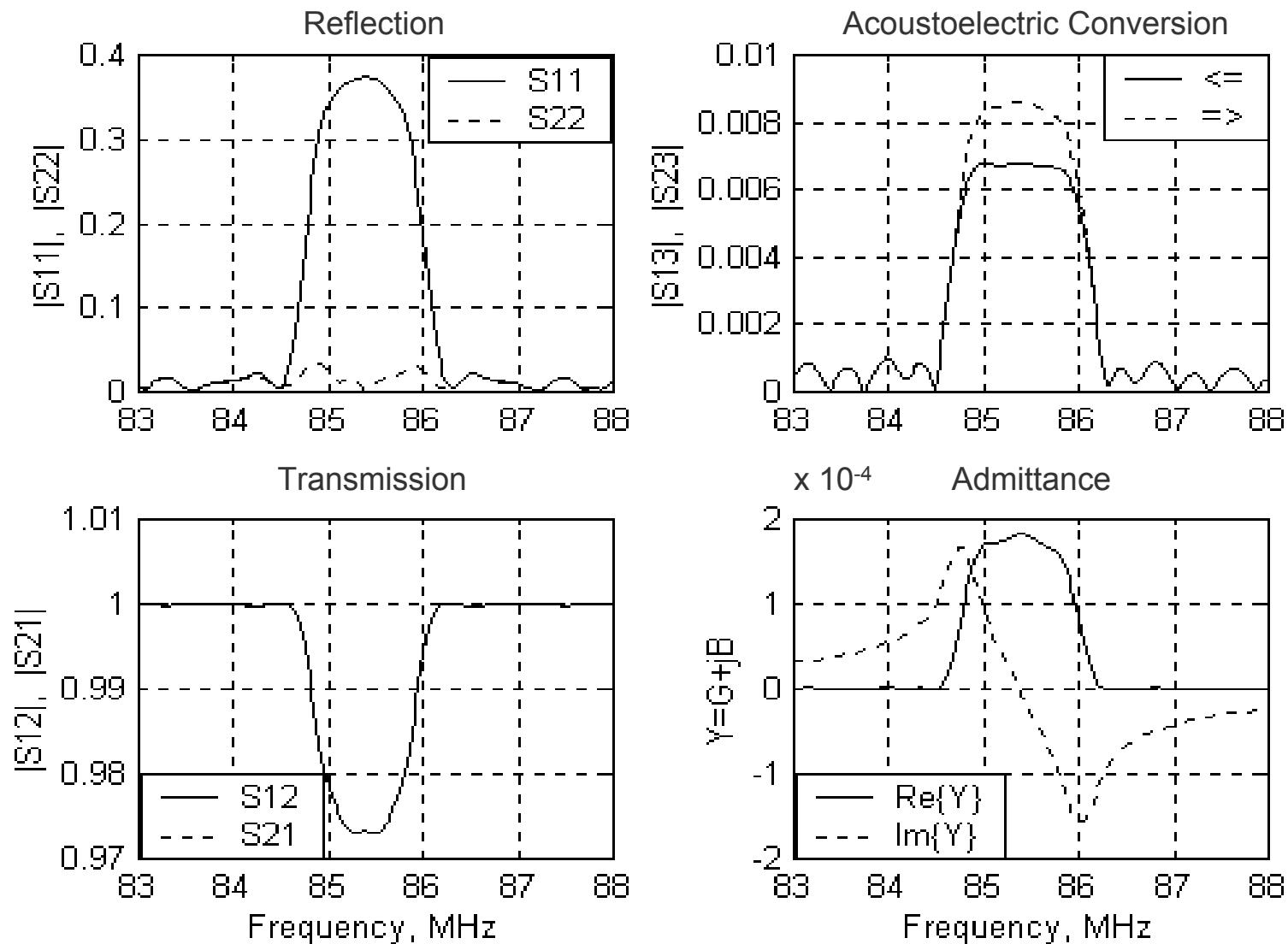


Fig. 11. Scattering parameters

Input SPUDT: Directivity

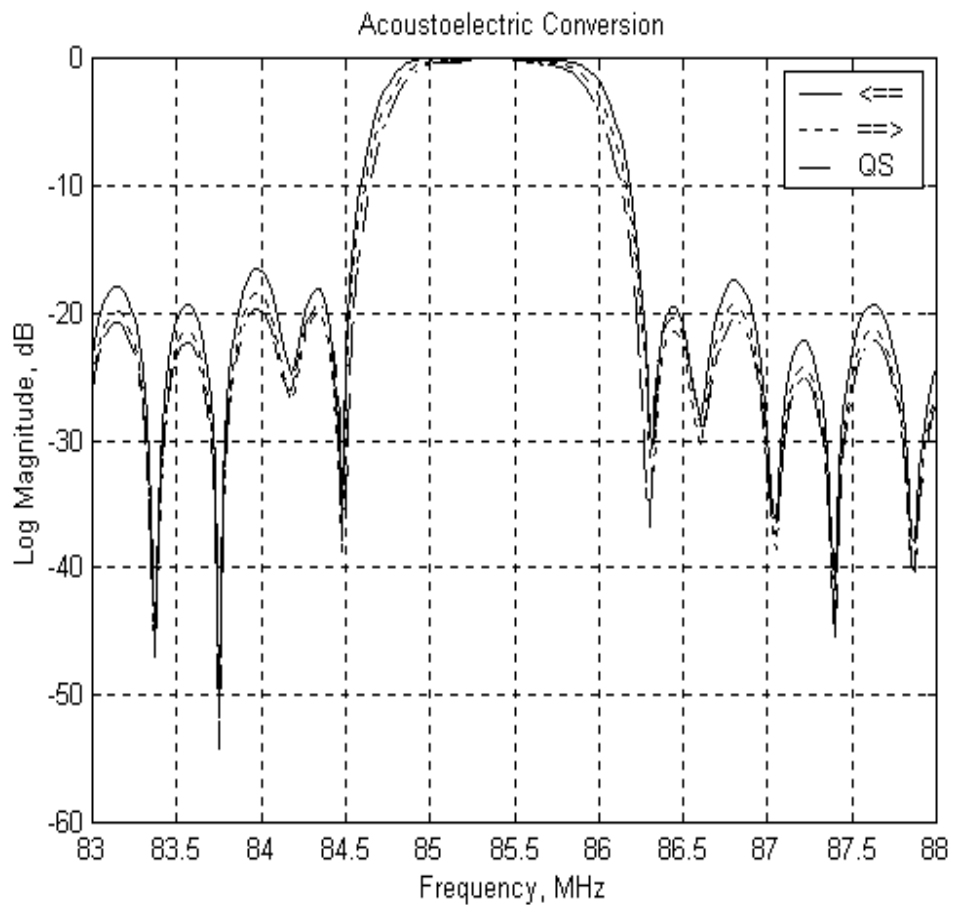


Fig. 12. Acoustoelectric conversion

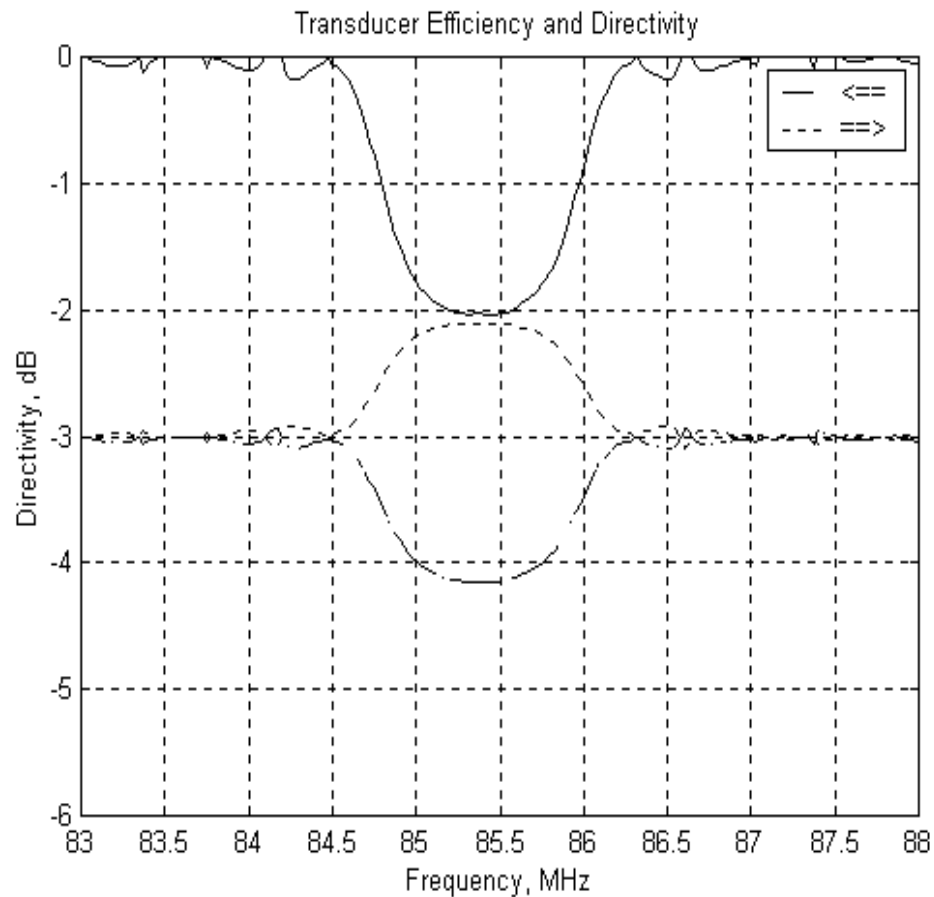
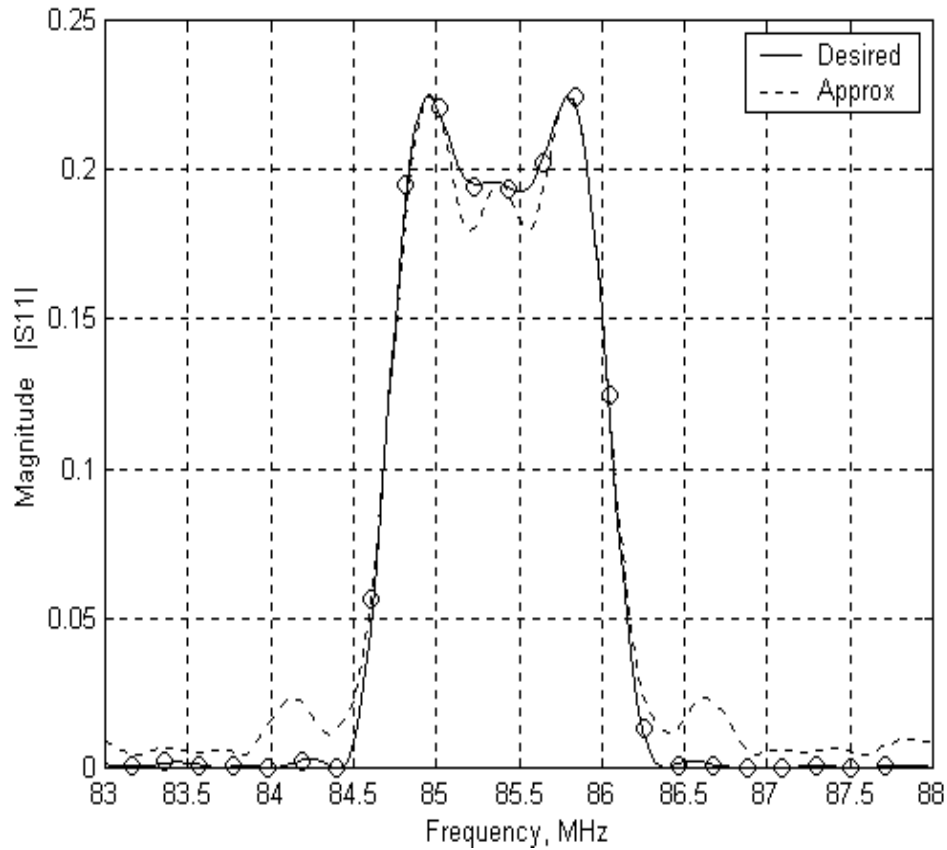
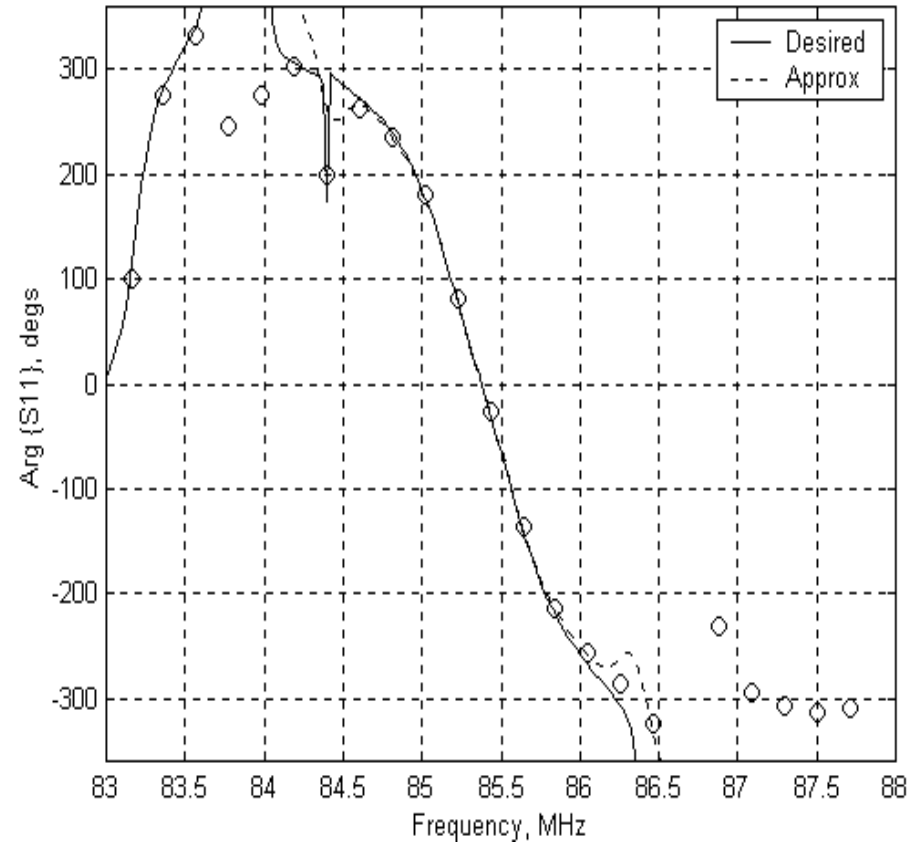


Fig. 13. Transducer directivity

Output SPUDT: Reflection



a) magnitude



b) phase

Fig. 14. Reflection function output SPUDT)

Output SPUDT: Scattering Parameters

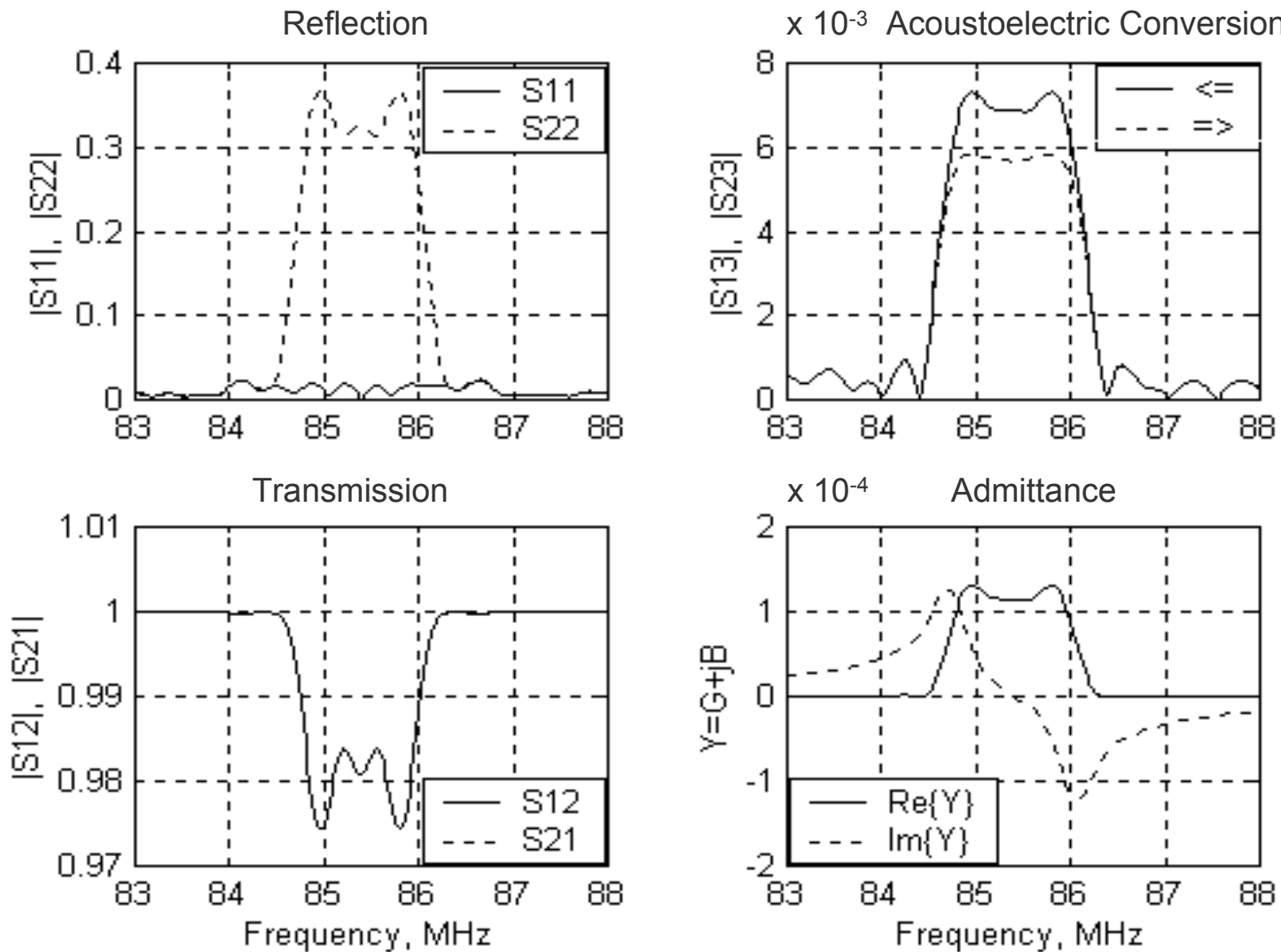


Fig. 15. Scattering parameters

Output SPUDT: Directivity

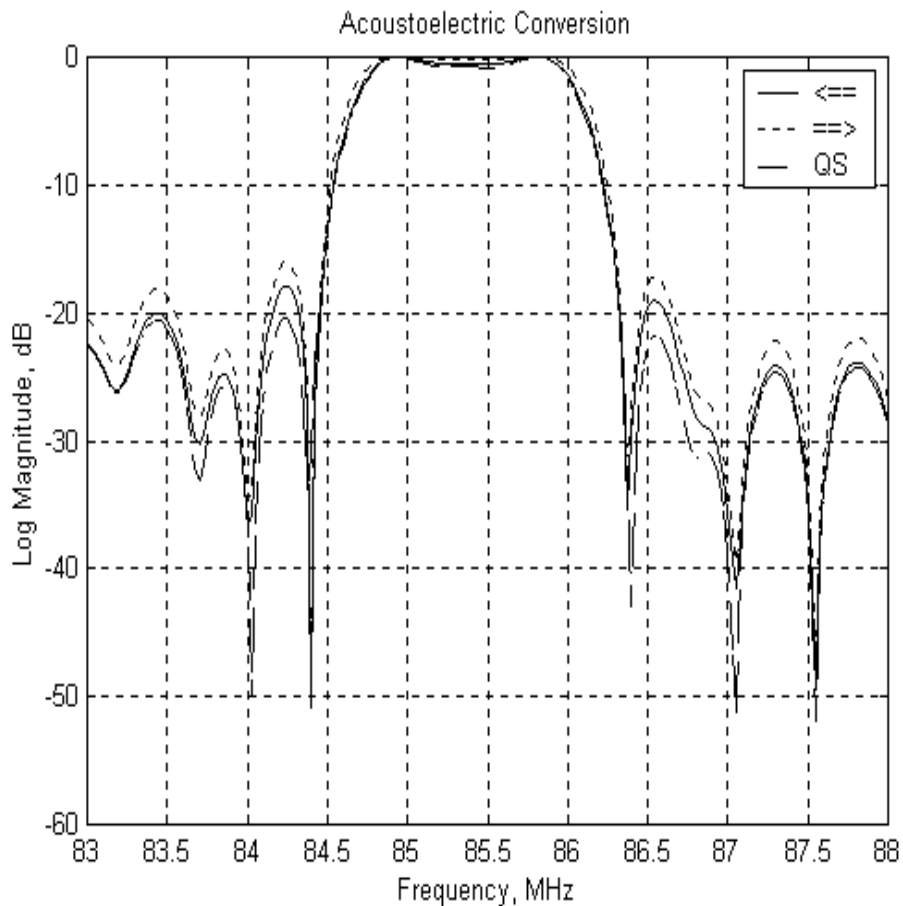


Fig. 16. Acoustoelectric conversion

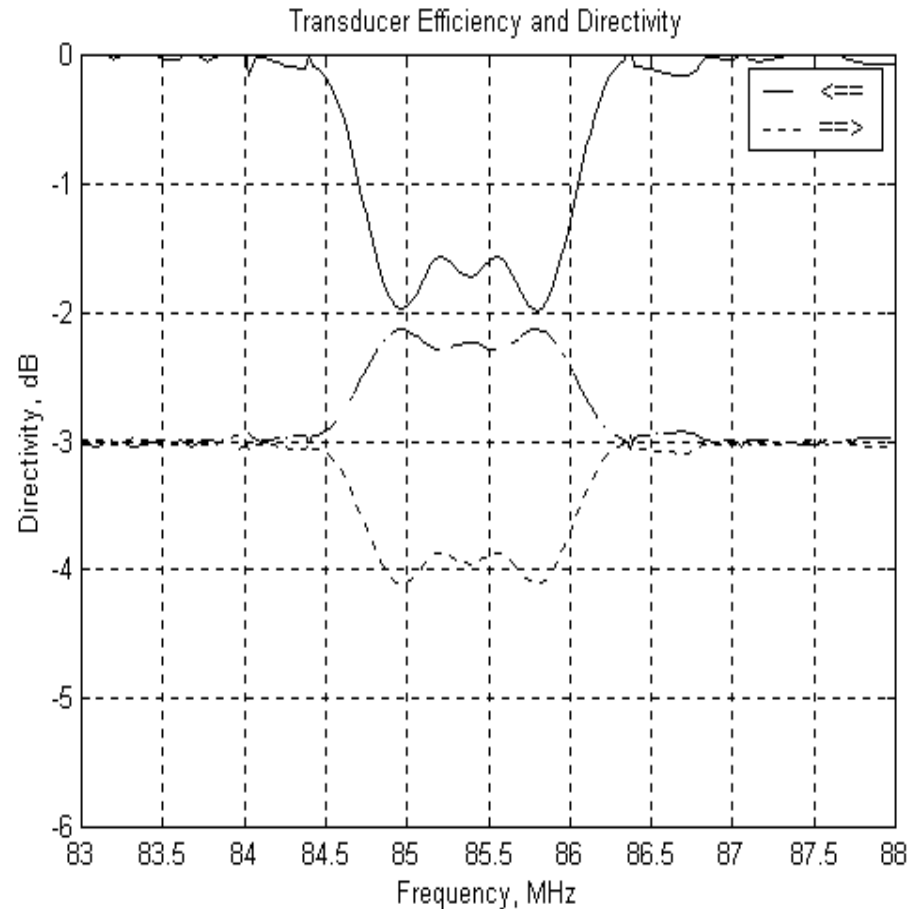
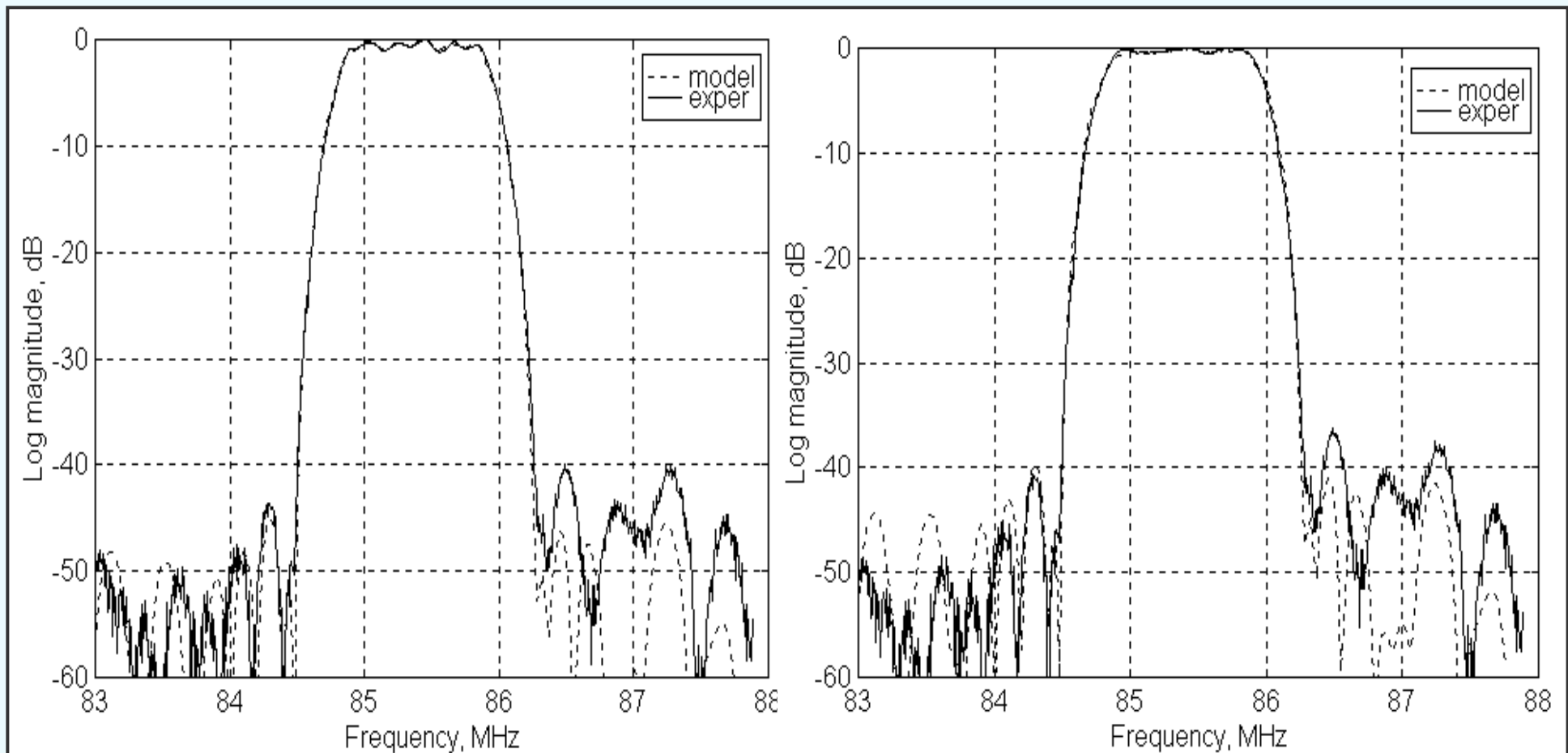


Fig. 17. Transducer directivity

Modeled and Experimental Results



a) unmatched

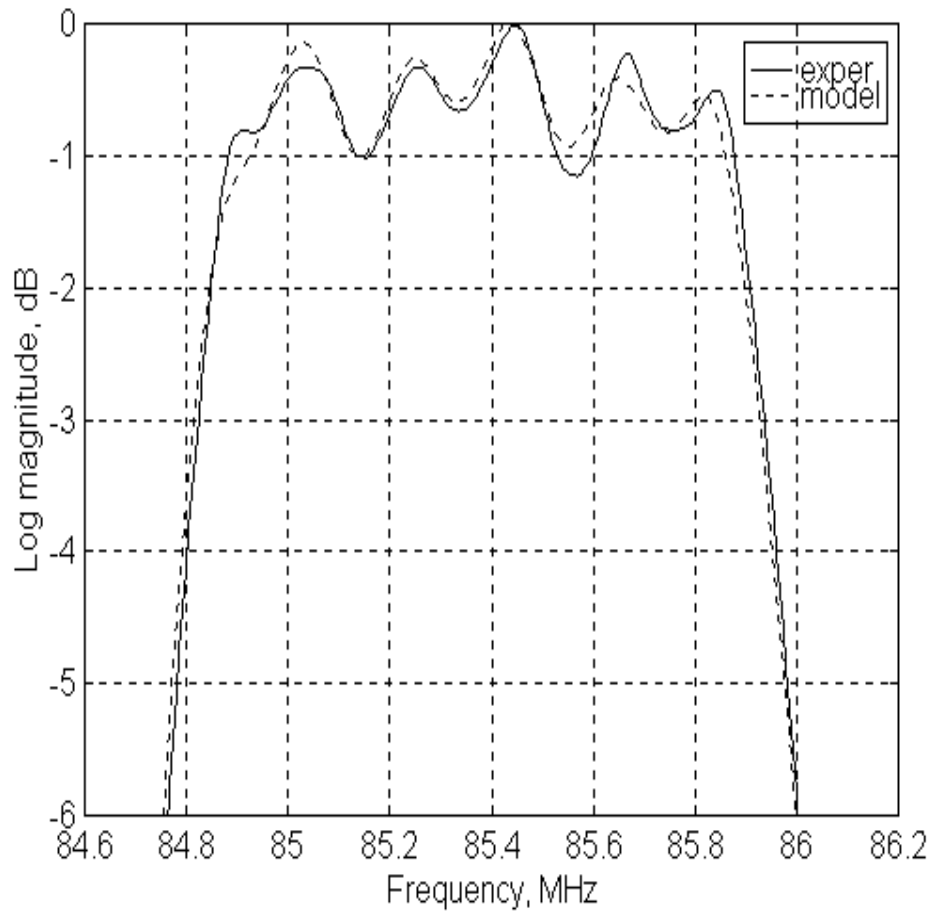
b) matched ($Q=40$)

Fig. 18. SAW filter response in 50- Ω system:

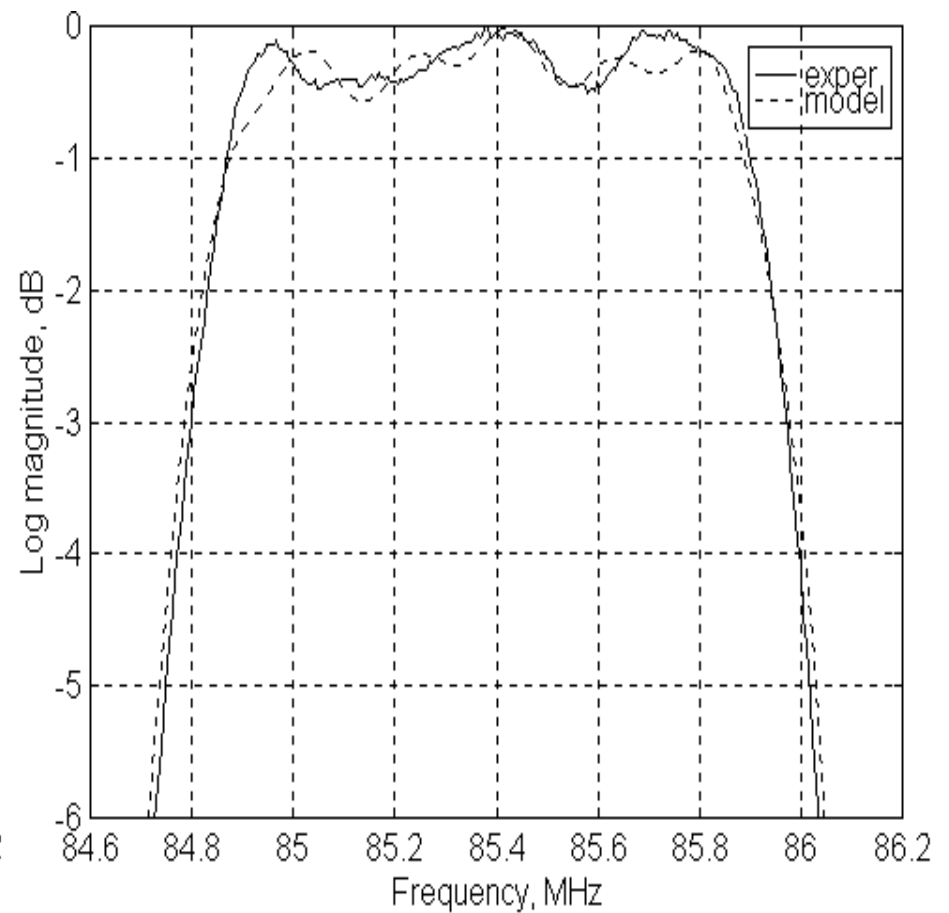
a) unmatched $IL=-35/36$ dB (modeled/measured);

b) matched $IL=-13/14$ dB (modeled/measured)

Modeled and Experimental Results (Pass Band)



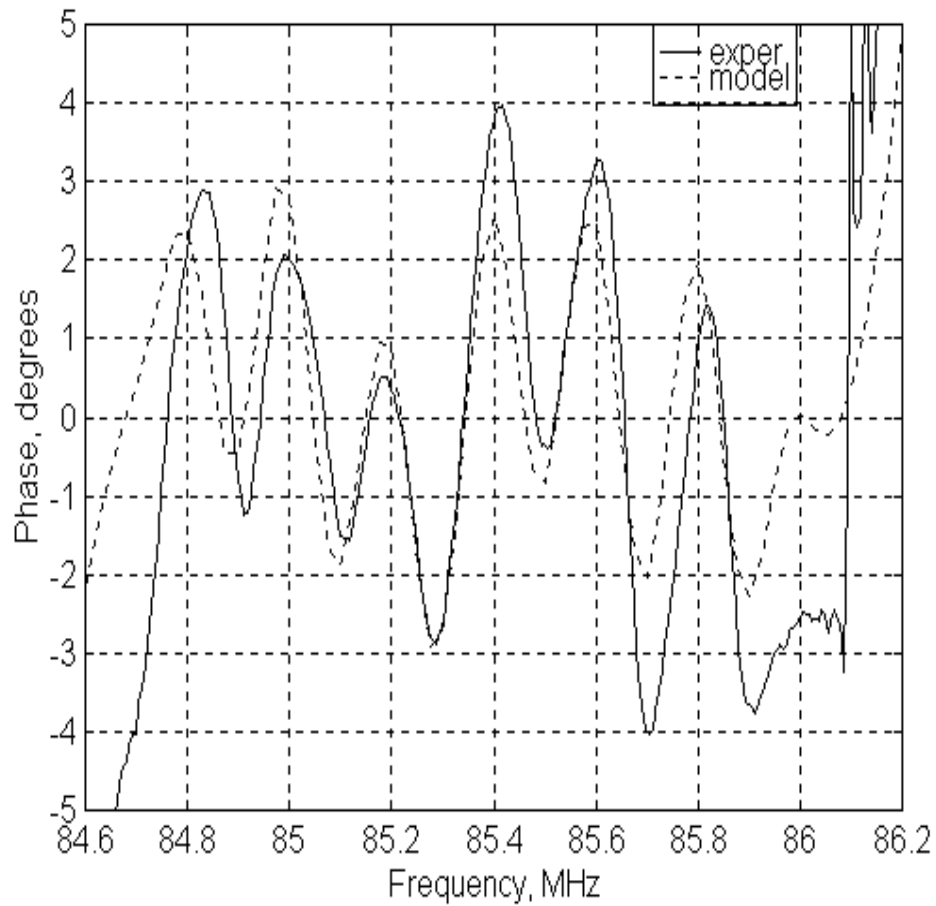
a) unmatched



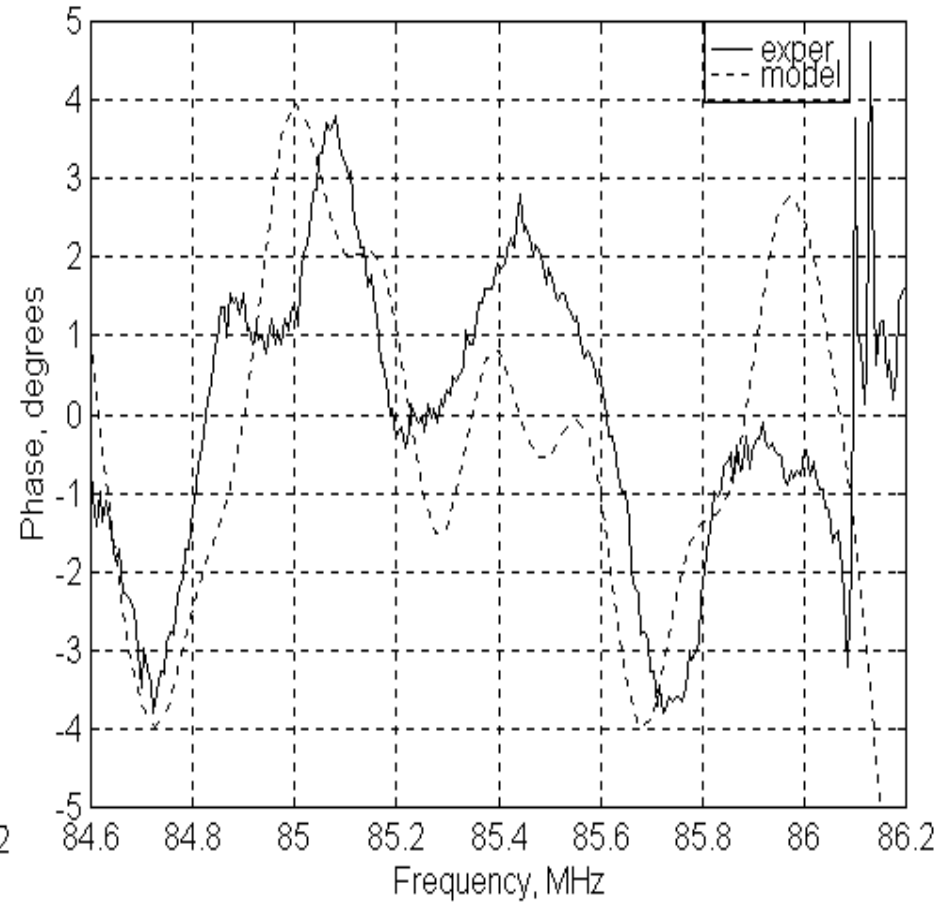
b) matched ($Q=40$)

Fig. 19. SAW filter magnitude response

Modeled and Experimental Results (Phase)



a) unmatched



b) matched ($Q=40$)

Fig. 20. SAW filter phase response

RSPUDT Optimization

For the given desired (target) bandpass frequency response

$$F_0(\omega) = R_0(\omega)e^{j\theta_0(\omega)} \quad (17)$$

where $R_0(\omega)$ is the magnitude response and $\theta_0(\omega)$ is the phase response we introduce separately the weighted Chebyshev magnitude, phase and optionally group delay error functions

$$\begin{aligned} E_R(\omega) &= W_R(\omega)[F(\omega) - R_0(\omega)] \\ E_\theta(\omega) &= W_\theta(\omega)[\theta(\omega) - \theta_0(\omega)] \\ E_\tau(\omega) &= W_\tau(\omega)[\tau(\omega) - \tau_0(\omega)] \end{aligned} \quad (18)$$

$\tau(\omega) = -\frac{d\theta}{d\omega}$ is the group delay response.

The non-linear Chebyshev (minimax) approximation problem:

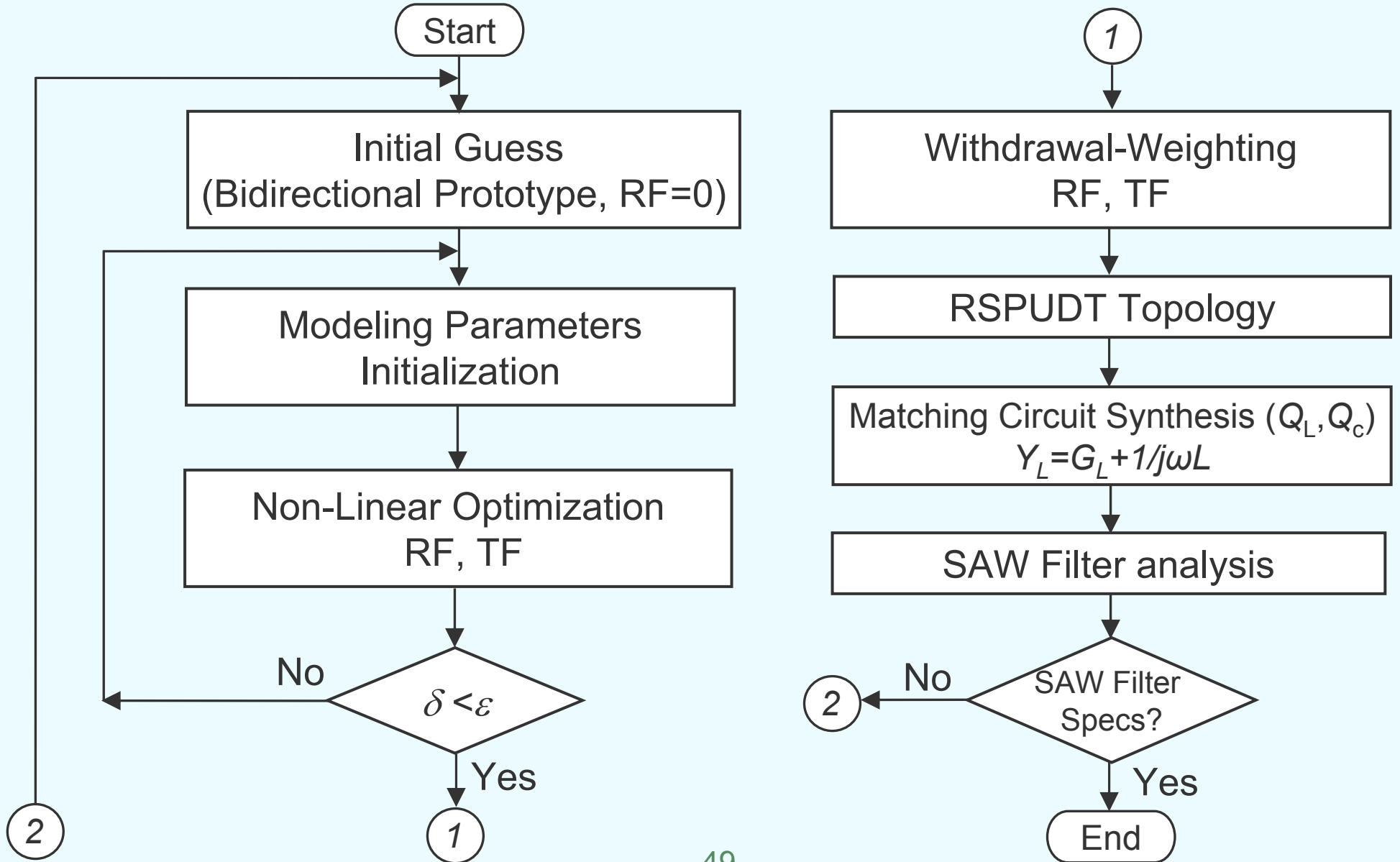
$$\delta = \min_{R,T} \left\{ \max_{\Omega} (E_R(\omega), E_\theta(\omega), E_\tau(\omega)) \right\} - ? \quad (19)$$

where R , T are the reflectivity and transduction (excitation) functions to be optimized.

Optimization Problem Features

1. The approximation function $F(\omega)=S_{12}(\omega)$ where the SAW filter transmission coefficient $S_{12}(\omega)$ (two-port) accounts for the matching circuits (matching impedances).
2. The optimized functions are both the *reflectivity* and *excitation* functions of the input and output SAW transducers and optionally the reflectivity function of the grounded grating to be placed in a spacer between transducers.
3. The optimized functions are base band converted and downsampled to reduce the number of the optimized variables.
4. The additional range constraints on the strip reflection coefficient, matching impedance, insertion loss, etc. can be introduced in the problem (19).
5. The optimization problem can be solved by standard methods of the non-linear constrained optimization.

RSPUDT Design Flowchart



RSPUDT Design Example

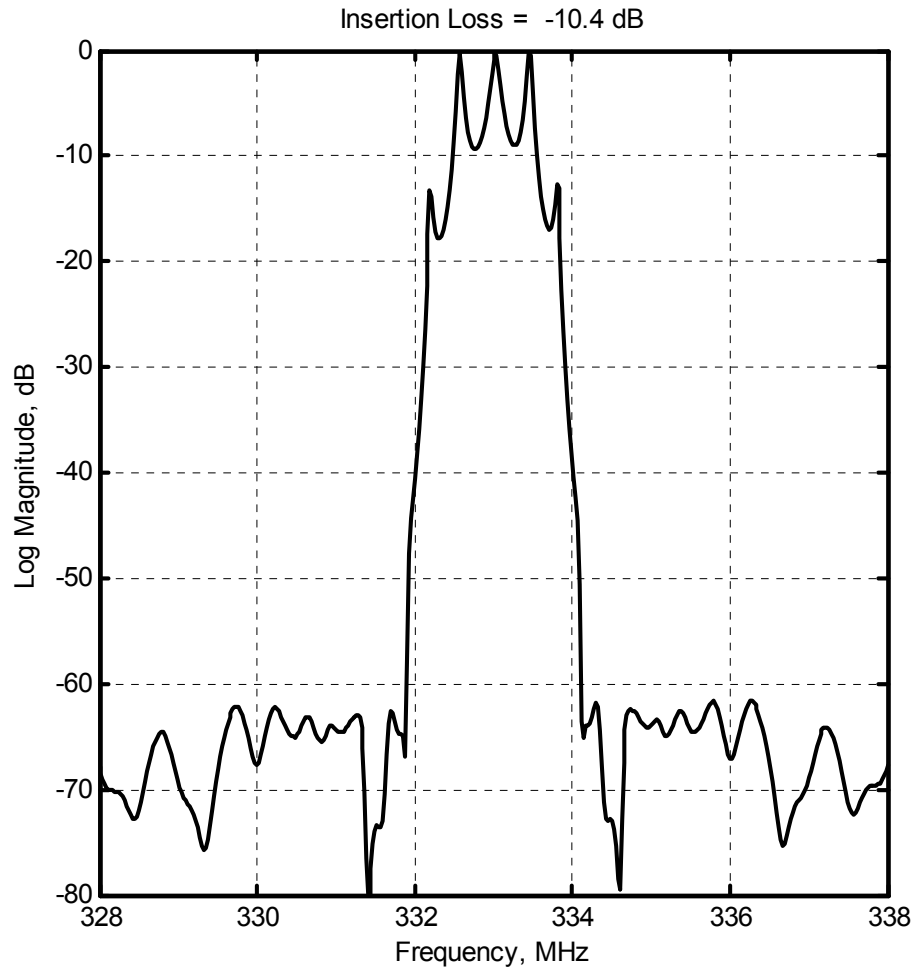
SAW Filter Specifications

Parameter	Unit	Min	Typ	Max	Note
Center Frequency f_o	MHz		333		
Insertion Loss at f_o	dB		6.5	8	Matched, Q=30
Passband Width	MHz		1.045		
-3 dB			1.850		
-20 dB			2.075		
-30 dB			2.20		
-40 dB			2.40		
-50 dB					
Relative Attenuation	dB		48		
$f_o - 50 \text{ MHz} \dots f_o - 3 \text{ MHz}$			48		
$f_o + 3 \text{ MHz} \dots f_o + 20 \text{ MHz}$			50		
$f_o + 20 \text{ MHz} \dots f_o + 40 \text{ MHz}$			50		
$f_o + 40 \text{ MHz} \dots f_o + 50 \text{ MHz}$					

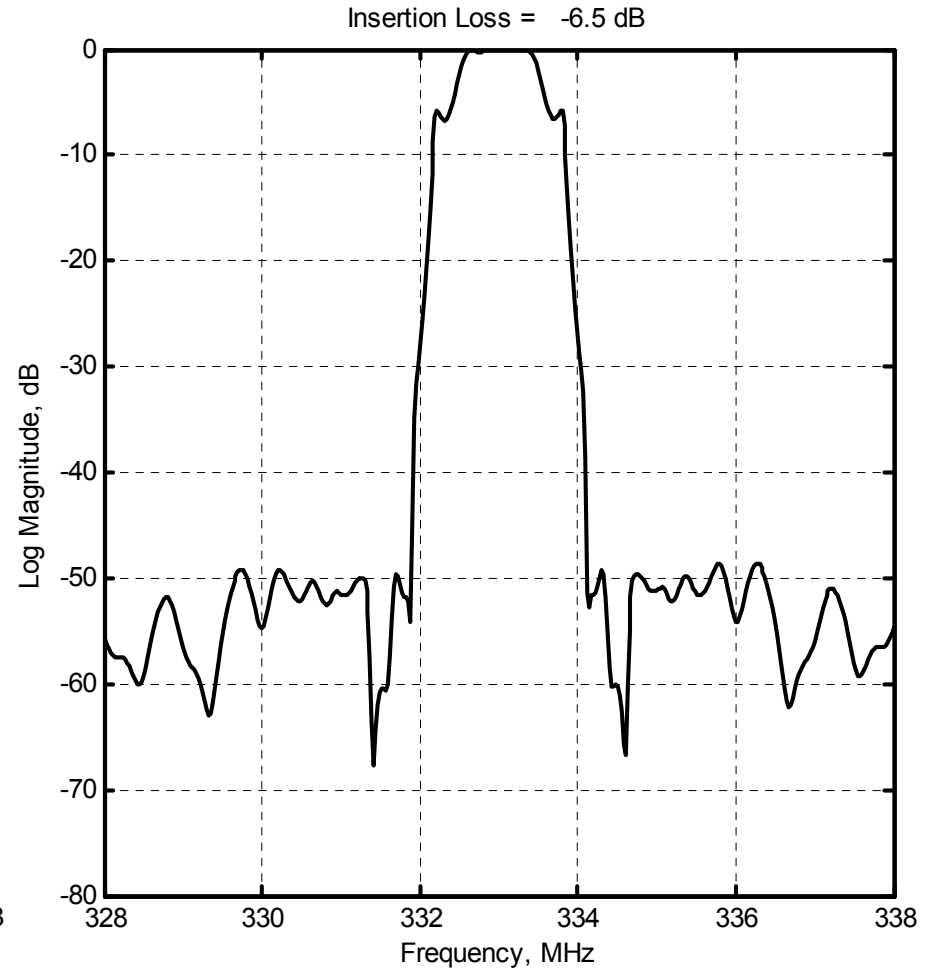
SAW Filter Specifications (Cont'd)

Parameter	Unit	Min	Typ	Max	Note
Passband Ripple	dB		0.5	1	At $f_o \pm 0.4$ MHz (p-p)
Group Delay Variation	nsecs		400	500	At $f_o \pm 0.4$ MHz (p-p)
Absolute Group Delay	μ sec		1.03		
Reflected Wave Signal Suppression	dB		55		13 ... 20 μ sec
Substrate Material			Quartz		
Temperature Coefficient of Frequency (TCF)*	ppm/ $^{\circ}$ C ²		-0.036		
Turnover Temperature	$^{\circ}$ C		15		
Operating Temperature	$^{\circ}$ C	-55	25	85	
Storage Temperature	$^{\circ}$ C	-55		85	
Package Size	mm		9.1 x 4.5		SMD

RSPUDT Modeled Results



a) unmatched



b) matched

Fig. 21. RSPUDT SAW filter magnitude response (simulation)

RSPUDT Modeled Results (Pass Band)

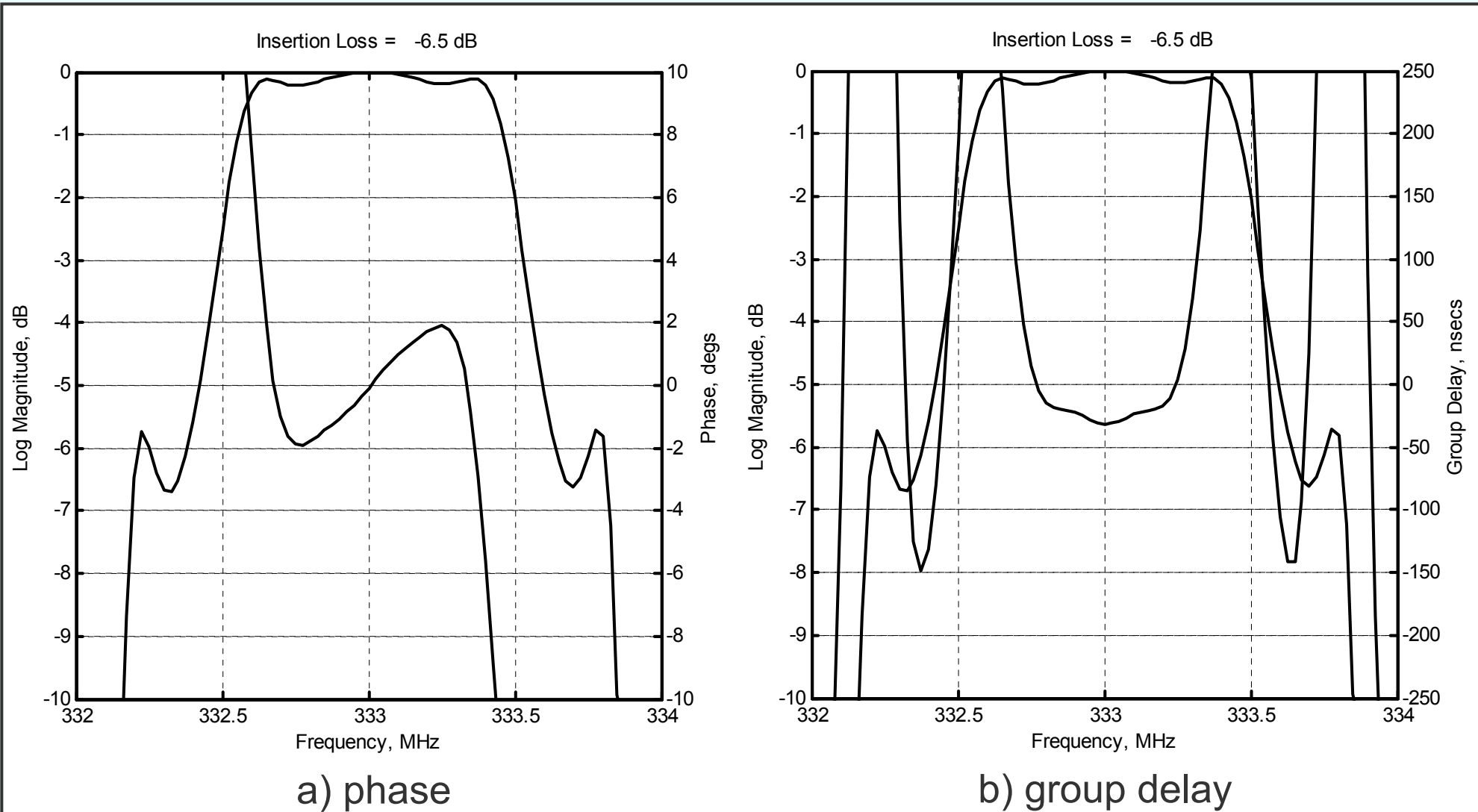


Fig. 22. RSPUDT SAW filter passband response (simulation)

RSPUDT SAW Filter Matching Circuit

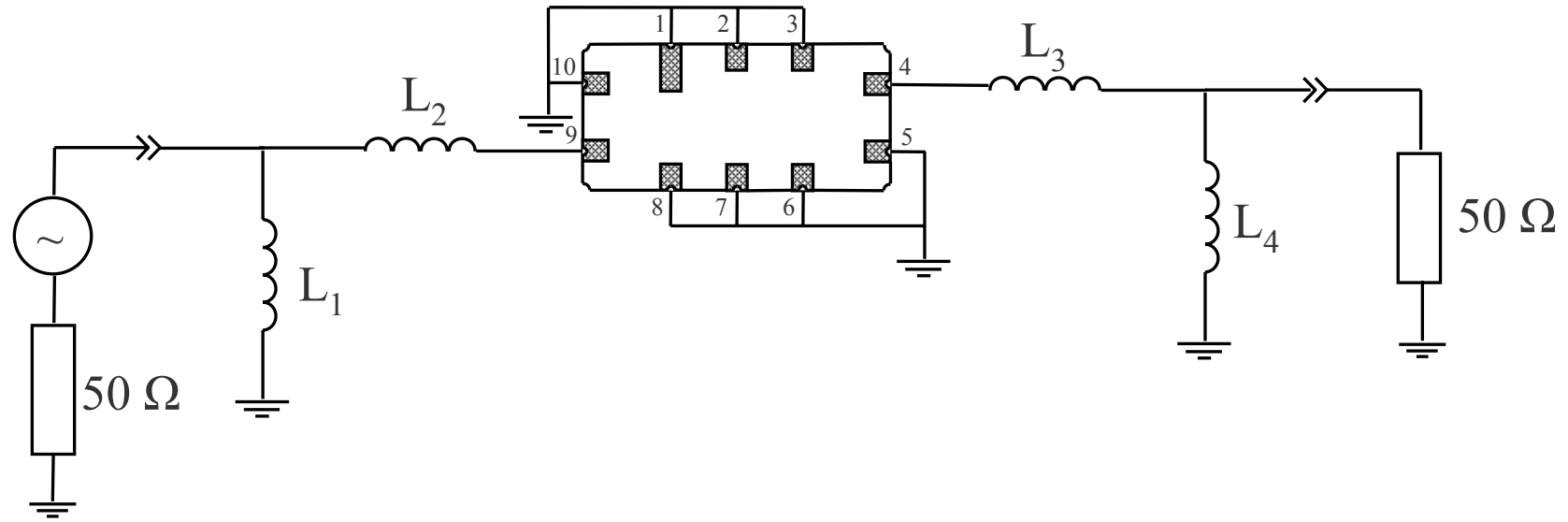


Fig. 23. Matching circuit configuration: $L_1= 8.2\ \text{nH}$, $L_2=15\ \text{nH}$, $L_3= 20\ \text{nH}$, $L_4=7.5\ \text{nH}$

RSPUDT SAW Filter Smith Chart (Matched)

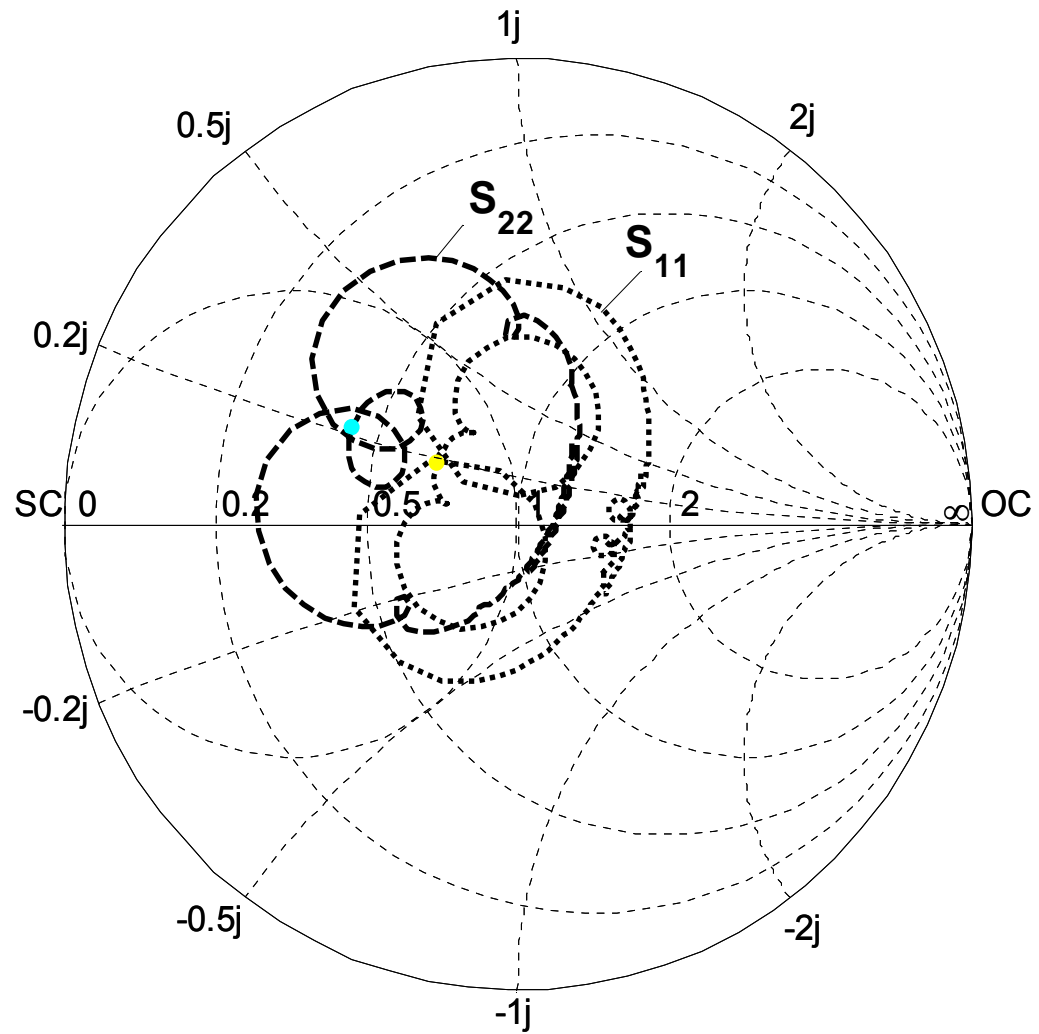


Fig. 24. Smith chart diagram

RSPUDT SAW Filter Time Response

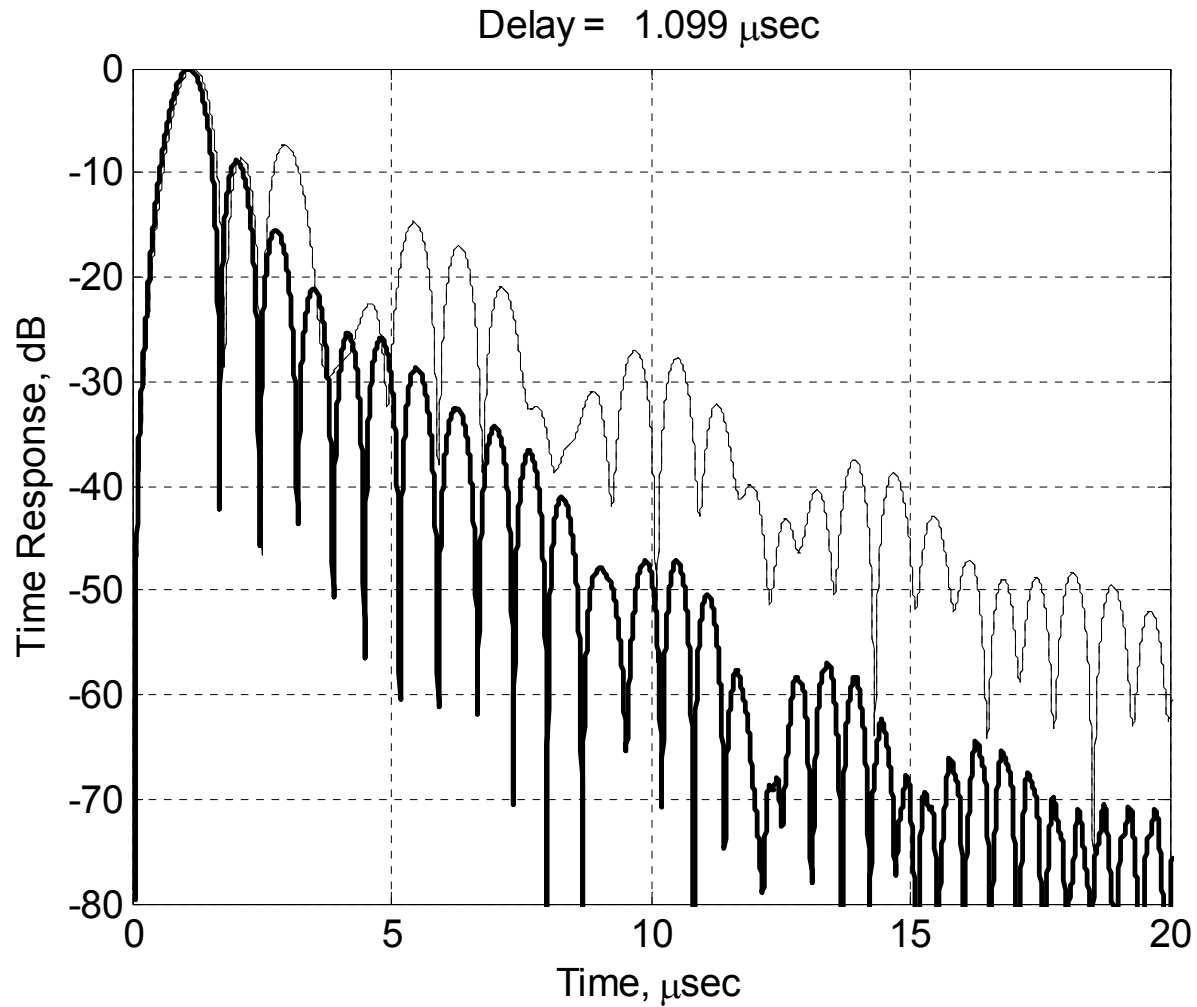


Fig. 26. RSPUDT SAW filter time response:
—— unmatched, —— matched)

Conclusions

SPUDT SAW Filters

- SPUDT SAW filters exploit internal mechanical reflections to cancel the regenerated signal at the forward acoustic port.
- To obtain the unidirectivity, the global or local reflection and transduction centers must be $\pm\lambda/8+n\lambda/2$ apart.
- When properly matched, SPUDT SAW filters have lower insertion loss at the smaller pass band ripple if compared to the bidirectional SAW filters due to the good TTE suppression.
- The design procedure of SPUDT SAW filters is based on the zero reflection condition at the forward acoustic port and must be performed iteratively, in general case.

Conclusions (Cont'd)

RSPUDT SAW Filters

- The resonant SPUDT (RSPUDT) have both the positive and negative reflections that allows to further reduce a SAW filter length and improve SAW filter performance.
- The sophisticated non-linear programming procedure must be applied to design RSPUDT SAW filters, with the input and output reflective and transduction functions optimized simultaneously.
- Design examples of the SPUDT and RSPUDT SAW filters are presented to confirm the modeling and design capabilities.

The End

Thanks for your attention.

Questions?